

Hyperstrong Radio-Wave Scattering in the Galactic Center. II. A Likelihood Analysis of Free Electrons in the Galactic Center

T. Joseph W. Lazio¹

Naval Research Laboratory, Code 7210, Washington, DC 20375-5351; lazio@rsd.nrl.navy.mil

and

James M. Cordes

Department of Astronomy and National Astronomy & Ionosphere Center,
Cornell University, Ithaca, NY 14853-6801;
cordes@spacenet.tn.cornell.edu

ABSTRACT

The scattering diameters of Sgr A* and several nearby OH masers ($\approx 1''$ at 1 GHz) indicate that a region of enhanced scattering is along the line of sight to the Galactic center. We combine radio-wave scattering data and free-free emission and absorption measurements in a likelihood analysis that constrains the following parameters of the GC scattering region: The GC-scattering region separation, Δ_{GC} ; the angular extent of the region, ψ_ℓ and ψ_b ; the outer scale on which density fluctuations occur, l_0 ; and the gas temperature, T_e . The maximum likelihood estimates of these parameters are $\Delta_{\text{GC}} = 133_{-80}^{+200}$ pc, $0.5^\circ \leq \psi_\ell \lesssim 1^\circ$, and $(l_0/1 \text{ pc})^{2/3} T_e^{-1/2} = 10^{-7 \pm 0.8}$. The parameter ψ_b was not well constrained and we adopt $\psi_b = 0.5^\circ$. The close correspondence between Δ_{GC} and $\psi_\ell D_{\text{GC}}$ suggests that the scattering region encloses the GC. As host media for the scattering, we consider the photoionized surface layers of molecular clouds and the interfaces between molecular clouds and the 10^7 K ambient gas. We are unable to make an unambiguous determination, but we favor the interface model in which the scattering medium is hot ($T_e \sim 10^6$ K) and dense ($n_e \sim 10 \text{ cm}^{-3}$). The GC scattering region produces a 1 GHz scattering diameter for an extragalactic source of $90''$, if the region is a single screen, or $180''$, if the region wraps around the GC, as appears probable. We modify the Taylor-Cordes model for the Galactic distribution of free electrons in order to include an explicit GC component. We predict that pulsars seen through this region will have a dispersion measure of approximately 2000 pc cm^{-3} , of which approximately 1500 pc cm^{-3} arises from the GC component itself. We stress the uniqueness of the GC scattering region, probably resulting from the high-pressure environment in the GC.

Subject headings: Galaxy:center — ISM:general — scattering

¹NRC-NRL Research Associate

1. Introduction

Davies, Walsh, & Booth (1976) established that the observed diameter of Sgr A*, the compact source in the Galactic center, scales as λ^2 , as expected if interstellar scattering from microstructure in the electron density determines the observed diameter. The observed diameter of Sgr A* is now known to scale as λ^2 from 30 cm to 3 mm (Rogers et al. 1994) and to be anisotropic at least over the wavelength range 21 cm to 7 mm (Backer et al. 1993; Krichbaum et al. 1993; Yusef-Zadeh et al. 1994). Maser spots in OH/IR stars within 25' of Sgr A* also show enhanced, anisotropic angular broadening (van Langevelde et al. 1992; Frail et al. 1994). These observations indicate that a region of enhanced scattering with an angular extent of at least 25' in radius (60 pc at 8.5 kpc) is along the line of sight to Sgr A*. At 1 GHz the level of angular broadening produced by this scattering region is roughly 10 times greater than that predicted by a recent model for the distribution of free electrons in the Galaxy (Taylor & Cordes 1993, hereinafter TC93), even though this model includes a general enhancement of scattering toward the inner Galaxy.

These observations do not constrain the *radial* location of the scattering region for the following reason: All previous observations have been of sources in or near the Galactic center, and for such sources, a region of moderate scattering located far from the Galactic center can produce angular broadening equivalent to that from a region of intense scattering located close to the Galactic center. Previous estimates for the location of the scattering region have ranged from 10 pc to 3 kpc. Ozernoi & Shisov (1977) concluded that an “unrealistic” level of turbulence is implied unless the region is within 10 pc of the Galactic center. The level of turbulence they considered unrealistic, however, namely $\sqrt{\langle n_e^2 \rangle} / \langle n_e \rangle \sim 1$, does appear to occur elsewhere in the interstellar medium (Spangler 1991). Further, van Langevelde et al. (1992) used the free-free absorption toward Sgr A* to constrain the region’s distance from the Galactic center to the range 0.85–3 kpc, though suitable adjustment of free parameters (outer scale and electron temperature) can decrease the limit to 0.03 kpc. We shall refer to the case in which the region is a site of extreme scattering, $\lesssim 100$ pc from the Galactic center and presumably caused by processes occurring there, as the GC model. We shall refer to the case in which the region is far from the GC, $\gtrsim 1$ kpc and a site of enhanced but not extreme scattering, as the random superposition (RS) model. Although the GC model is attractive for phenomenological reasons, other sites of enhanced interstellar scattering are found throughout the Galaxy (e.g., NGC 6634, Moran et al. 1990; Cyg X-3, Molnar et al. 1995) and the mean free path for encountering such a region is approximately 8 kpc (Cordes et al. 1991).

Identifying the location of the scattering is important in establishing the origin of the scattering. Associating the scattering with a specific region may elucidate the mechanism for the generation of the density fluctuations responsible for the scattering. The currently favored mechanism is that velocity or magnetic field fluctuations—or both—generate the density fluctuations (Higdon 1984, 1986; Montgomery, Brown, & Matthaeus 1987; Spangler 1991; Sridhar & Goldreich 1994; Goldreich & Sridhar 1995). Velocity or magnetic field fluctuations are also a natural means for inducing anisotropy in the density fluctuations and thereby in the scattering disks. If this mechanism is correct, the amplitude of the density fluctuations may provide a measure of the coupling between

the density and velocity or magnetic field fluctuations or, more generally, provide information about the small-scale velocity or magnetic field in the scattering region. However, current observational constraints are uncertain by the ratio of the Galactic center-scattering region distance to the Galactic center-Sun distance. In the RS model, the ratio is a few while in the GC model the ratio could be as large as one hundred, so the location of the scattering region is a key free parameter.

The location of the scattering region also has implications for pulsar searches toward the GC. Cordes & Lazio (1997) showed that even if the RS model is correct, pulsars seen through the scattering region will suffer pulse broadening of at least 5 s at 1 GHz (see also Davies et al. 1976a; Ozernoi & Shishov 1977). If the GC model is correct, only at frequencies above 10 GHz will pulsations be detectable (because of the ν^{-4} dependence of pulse broadening) and then only for pulsars with periods longer than 100 ms.

In this paper we develop a likelihood analysis to quantify the most probable Δ_{GC} for the scattering region. In §2 we describe our model for the distribution of free electrons in the GC. In §3 we assemble measurements from the literature relevant to radio-wave scattering and develop a likelihood method to constrain the properties of the scattering region, and in §4 we discuss our results and present our conclusions.

2. Electron Density Model for the Galactic Center

The TC93 model synthesized scattering measurements of pulsars, masers, and extragalactic sources and dispersion measurements of pulsars with independently known distances. This model for the global distribution of free electrons in the Galaxy does not include the enhanced scattering toward the GC, though TC93 acknowledged its existence and recognized this deficiency in the model. Their model underpredicts the angular broadening of Sgr A* and nearby sources by about a factor of 10 at 1 GHz. In this section we augment the TC93 model by considering the distribution of free electrons in the GC (see also §4.3).

For the GC region, the simplest model is one that can account for the following:

1. Comparable, large angular broadening of Sgr A* and OH/IR masers to at least about $30'$ away from Sgr A* (van Langevelde et al. 1992; Frail et al. 1994; Yusef-Zadeh et al. 1994);
2. Strong free-free emission and absorption within the Sgr A complex extending to approximately $5'$ from Sgr A* (Pedlar et al. 1989; Anantharamaiah et al. 1991);
3. Weak free-free emission and absorption over a wider region, of order $10'$, that includes the OH/IR masers (Anantharamaiah et al. 1991); and
4. Free-free absorption of Sgr A* at frequencies below about 0.9 GHz with an optical depth of unity in the frequency range 0.8–1 GHz (Davies et al. 1976a; Beckert et al. 1996).

To account for these observations with the simplest model, we consider thermal free electrons distributed in two main components: (1) a central spheroid of radius R_c centered on Sgr A*, and (2) a screen at distance Δ_{GC} from Sgr A*. Figure 1 shows other geometries for the scattering region that may be appropriate for the GC model; we can approximate the scattering region by a screen because of the weighting factor $\Delta_{\text{GC}}/D_{\text{GC}}$, where D_{GC} is the Galactic center-Sun distance (see below). In the GC model, the portion of the scattering region closest to the Earth will make the largest contribution to the scattering.

We assume the electron density fluctuations have a spatial power spectrum of the form (Coles et al. 1987)

$$P_{\delta n_e}(q, z) = C_n^2(z) q^{-\alpha} e^{-(ql_1/2)}, \quad (1)$$

for spatial wavenumbers $q \gg q_0 = 2\pi/l_0$. The outer and inner scales to the density spectrum are $l_{0,1}$, respectively, and $C_n^2(z)$ is assumed to vary slowly along the line of sight. We include the inner scale in our description of the spectrum because Sgr A* is one of a small number of lines of sight for which an inner scale may have been detected (Spangler & Gwinn 1990). The more conventional power-law description, $P_{\delta n_e} \propto q^{-\alpha}$ (Rickett 1990; Armstrong, Rickett, & Spangler 1995; and references within) is obtained for wavenumbers $q_0 \ll q \ll q_1 = 2\pi/l_1$. We shall also henceforth assume that the spectral index of the spectrum is $\alpha = 11/3$, the Kolmogorov value, as suggested by a number of observations (Rickett 1990).

A point source in the Galactic center viewed through the scattering region, at a frequency of ν_{GHz} GHz, has an apparent diameter of (van Langevelde et al. 1992)

$$\theta_s = 133 \text{ mas} \nu_{\text{GHz}}^{-2} \left(\frac{l_1}{100 \text{ km}} \right)^{(4-\alpha)/2} \left[\int_0^D C_n^2(z) \left(\frac{z}{D} \right)^2 dz \right]^{1/2}. \quad (2)$$

The integral is taken from the source to the observer. The factor $(z/D)^2$ in equation (2) is the cause of the aforementioned distance ambiguity (Lee 1977; Ozernoi & Shishov 1977; Cordes, Weisberg, & Boriakoff 1985; van Langevelde et al. 1992). In contrast the scattering diameter of a compact extragalactic source viewed through this scattering region is (van Langevelde et al. 1992)

$$\theta_{\text{xgal}} = \frac{D_{\text{GC}}}{\Delta_{\text{GC}}} \theta_{\text{Gal}}, \quad (3)$$

where θ_{Gal} is the characteristic diameter of a GC source—the diameter of Sgr A* at 1 GHz is $1.^{\prime\prime}3$ —and we take the GC-Sun distance to be $D_{\text{GC}} = 8.5$ kpc (at this distance $1' = 2.5$ pc). Figure 2 shows θ_{xgal} as a function of Δ_{GC} . If the RS model is correct and $\Delta_{\text{GC}} \gtrsim 1$ kpc, we expect extragalactic source diameters to be a few arcseconds; if the GC model is correct and $\Delta_{\text{GC}} \approx 100$ pc, source diameters could exceed 1 arc min . However, few extragalactic sources have been identified toward the GC. The two closest sources are B1739–298 (Dickey et al. 1983) and GPSR 0.539+0.263 (Bartel 1994, private communication), which are $48'$ and $40'$ from Sgr A*, respectively. Neither of these is within the region of enhanced scattering defined by the OH masers. Our observations of the GC (Lazio & Cordes 1997, hereinafter Paper I) revealed an apparent deficit of sources within

approximately 1° of Sgr A*, suggestive of extragalactic sources being broadened enough to be resolved out by our observations.

To describe the free electron density and its fluctuations, we use the conventional line-of-sight measures, EM, DM, and SM (Cordes et al. 1991). For simplicity, we consider the statistics of the electron density to be homogeneous in both components. We consider the electron density to be large in “cloudlets” in which the mean density is \bar{n}_e and that these cloudlets have volume filling factor f . Within a cloudlet, the fluctuations in n_e have an rms value $\varepsilon \equiv \delta n_e / \bar{n}_e$. For a path length L through a medium, the three measures are

$$\begin{aligned} DM &= fL\bar{n}_e \\ EM &= fL\bar{n}_e^2(1 + \varepsilon^2) = \bar{n}_e DM (1 + \varepsilon^2) \\ SM = C_{\text{SM}} l_0^{3-\alpha} f L \bar{n}_e^2 \varepsilon^2 &= C_{\text{SM}} l_0^{3-\alpha} \bar{n}_e \varepsilon^2 DM = C_{\text{SM}} l_0^{3-\alpha} EM \left[\frac{\varepsilon^2}{(1 + \varepsilon^2)} \right], \end{aligned} \quad (4)$$

where $C_{\text{SM}} \equiv (\alpha - 3)/2(2\pi)^{4-\alpha}$ is a constant and α is the spectral index of the density spectrum, equation (1).

For the two components, the following general constraints are built into our likelihood analysis:

Central Component: From emission and absorption measurements, we obtain the radius R_c ($\approx 5'$) and the emission measure $EM_c(T_c)$ as a function of temperature, T_c . From EM_c we can calculate DM_c and SM_c using the above relations.

Screen: Assume a thickness $\Delta d_s \ll \Delta_{\text{GC}} \ll D_{\text{GC}}$. From angular diameter observations of Sgr A*, OH/IR masers, and the GC transients, we determine the angular extent of the screen ($\gtrsim 15'$) and the total scattering measure as a function of Δ_{GC} . We argue that the GC scattering is dominated by the scattering measure of the screen, SM_s . From SM_s , we can derive DM_s and EM_s .

The overall constraints are that the total emission measure,

$$EM = EM_c + EM_s, \quad (5)$$

must be dominated by the central spheroid component, since absorption and strong emission are not seen beyond the GC spheroid, while the weighted scattering measure

$$\begin{aligned} \mathcal{S}(\Delta_{\text{GC}}) &= \int ds \left[C_{n,c}^2(s) + C_{n,s}^2(s) \right] \left(\frac{s}{D_{\text{GC}}} \right)^2 \\ &\approx \frac{1}{3} SM_c \left(\frac{R_c}{D_{\text{GC}}} \right)^2 + SM_s \left(\frac{\Delta_{\text{GC}}}{D_{\text{GC}}} \right)^2 \end{aligned} \quad (6)$$

is dominated by the screen, since lines of sight that do not intersect the spheroid (i.e., those toward some of the OH/IR masers) show angular broadening at least as strong as the line of sight toward Sgr A*.

The most important parameters of this model that we wish to constrain are

1. Δ_{GC} , the distance of scattering screen from Sgr A*;
2. ψ_ℓ and ψ_b , the angular extent of the scattering screen in the ℓ and b directions;
3. l_0 , the outer scale of electron density fluctuations in the screen, and
4. T_e , the temperature of the gas responsible for the scattering.

3. Likelihood Functions for Galactic Center Scattering

The measurements available for constraining scattering in the GC consist of broadening observations of OH masers, source counts, and free-free emission and absorption. The joint likelihood function for these scattering measurements is

$$\begin{aligned} \mathcal{L} &= \mathcal{L}(\theta_{\text{OH}}, N, T_{\text{ff}}, \tau_{\text{ff}} | \Delta_{\text{GC}}, \psi_\ell, \psi_b, l_0, T_e) \\ &= \mathcal{L}(T_{\text{ff}}, \tau_{\text{ff}} | \theta_{\text{OH}}, N; \Delta_{\text{GC}}, \psi_\ell, \psi_b, l_0, T_e) \mathcal{L}(N | \theta_{\text{OH}}; \Delta_{\text{GC}}, \psi_\ell, \psi_b) \mathcal{L}(\theta_{\text{OH}} | \Delta_{\text{GC}}, \psi_\ell, \psi_b) \\ &= \mathcal{L}_{\text{ff}} \mathcal{L}_{\text{counts}} \mathcal{L}_{\text{broaden}}. \end{aligned} \quad (7)$$

The various factors in this expression are

$\mathcal{L}_{\text{broaden}} = \mathcal{L}(\theta_{\text{OH}} | \Delta_{\text{GC}}, \psi_\ell, \psi_b)$ is the likelihood function for angular broadening measurements of sources in and near the GC. In principle we have available measurements of OH masers (van Langevelde & Diamond 1991; van Langevelde et al. 1992; Frail et al. 1994), H₂O masers (Gwinn et al. 1988), the GC transients (Davies et al. 1976b; Zhao et al. 1992), and extragalactic sources (Paper I; Bartel 1996, private communication). In practice we shall restrict our attention to the OH masers, $\mathcal{L}_{\text{broaden}} = \mathcal{L}_{\text{OH}}$. Thus far, only OH masers and the transients have been found behind the screen. For the OH/IR star population the three-dimensional spatial distribution in the GC has been inferred. We will transform this spatial distribution into a distribution of scattering diameters. A similar technique cannot be utilized for the transients because the spatial distribution of the underlying population is not known.¹ Should this distribution become known, a similar procedure could be used to include an additional factor in $\mathcal{L}_{\text{broaden}}$. As there are currently only two known transients, both within 1' of Sgr A*, their contribution to $\mathcal{L}_{\text{broaden}}$ would not be substantial. Although no H₂O masers or extragalactic sources with measured angular diameters have been seen

¹ Neutron-star or black-hole binaries are probably responsible for these radio transients. These systems also appear as X-ray sources and the spatial distribution of X-ray sources toward the GC has been inferred (Skinner 1993). The radio transient discovered by Davies et al. (1976b) was indeed determined to be positionally coincident with an X-ray source. No such identification was made for the radio transient discovered by Zhao et al. (1992).

through the screen, these classes of sources can still be used to place limits on the angular extent of the screen.

$\mathcal{L}_{\text{counts}} = \mathcal{L}(N|\theta_{\text{OH}}; \Delta_{\text{GC}}, \psi_\ell, \psi_b)$ is the *conditional* likelihood function for counts of individual sources in our VLA fields (Paper I). We shall concentrate on our fields because they are larger and deeper than those from the Columbia Plane Survey (Zoonemerkermani et al. 1990; Helfand et al. 1992; hereinafter the CPS).

$\mathcal{L}_{\text{ff}} = \mathcal{L}(T_{\text{ff}}, \tau_{\text{ff}}|\theta_{\text{OH}}, N; \Delta_{\text{GC}}, \psi_\ell, \psi_b, l_0, T_e)$ is the *conditional* likelihood function for free-free emission and absorption measurements.

In the remaining sections, we describe each factor in \mathcal{L} , including the relevant data, derivation of the likelihood factor, the parameters of the factor, and the results for that factor. We then combine these likelihoods to form the global likelihood.

3.1. Angular Broadening

3.1.1. Data

We summarize previous angular broadening measurements for sources toward the GC in Table 1, scaling the reported angular diameter to 1 GHz assuming a λ^2 scaling, as is appropriate for extreme scattering (van Langevelde et al. 1992); the distribution of scattering diameters is shown in Fig. 3. As discussed above, we shall focus on the OH/IR stars.

Lindqvist, Habing, & Winnberg (1992) determined the three-dimensional distribution of a sample of 130 OH/IR stars; about one-half of the OH/IR stars for which scattering diameters have been determined are in this sample. They found the angular distribution of OH/IR stars to be elongated in ℓ with an ellipticity of 0.7–0.9 and the spatial density of OH/IR stars to be consistent with that of an isothermal sphere, $n \propto r^{-2}$, with a centroid near the position of Sgr A* (and IRS 16). This distribution will enable us to derive a likelihood function for individual OH/IR stars, a function which will depend on Δ_{GC} and the angular extent of the screen.

3.1.2. Likelihood Factor $\mathcal{L}_{\text{broaden}}$

We model the OH/IR star distribution with the cylindrically symmetric form

$$f_{r,\phi,z}(r, \phi, z) dr d\phi dz = \frac{\eta}{2\pi a_r^2 a_z \left[1 + (r/a_r)^2 + (z/a_z)^2 \right]} 2\pi r dr d\phi dz, \quad (8)$$

where a_r and a_z are the scales in the distribution and η is a numerical factor of order unity. Should the OH/IR stars have a bar-like distribution, then there would be a ϕ dependent term in equation (8).

Assume that the location of the scattering region may be described by its location $X_s(\ell, b)$ from the GC along an x -coordinate axis directed from Sgr A* to the Sun. The y -axis points toward $\ell = 270^\circ$ and the z -axis points out of the Galactic plane. For a radio source in the direction ℓ, b at radius r and angle ϕ from the x axis, the source-screen distance is then

$$\Delta = X_s(\ell, b) - r \cos \phi. \quad (9)$$

Using $y = r \sin \phi = D_{\text{GC}} \sin \ell$, the radius is $r = \sqrt{(X_s - \Delta)^2 + (D_{\text{GC}} \sin \ell)^2}$ and the transformation of the distribution in (r, ϕ, z) to one in Galactic coordinates and source-screen distance is

$$f_{\ell, b, \Delta}(\ell, b, \Delta) = \left(\frac{D_{\text{GC}}^2}{r} \right) f_{r, \phi, z}(r, \phi, z). \quad (10)$$

When calculating geometrical effects, we consider the screen to be infinitesimally thin. In this limit, we envision three simple shapes for the scattering screens, cf. Fig. 1:

flat screen: perpendicular to the line of sight to Sgr A* and at a distance Δ_{GC} from Sgr A*, for which

$$\begin{aligned} \Delta &= \Delta_{\text{GC}} - r \cos \phi, \\ X_s &= \Delta_{\text{GC}}; \end{aligned} \quad (11)$$

cylindrical screen: with radius Δ_{GC} coaxial with the z axis:

$$\begin{aligned} \Delta &= \left[\Delta_{\text{GC}}^2 - (D_{\text{GC}} \sin \ell)^2 \right]^{1/2} - r \cos \phi, \\ X_s &= \left[\Delta_{\text{GC}}^2 - (D_{\text{GC}} \sin \ell)^2 \right]^{1/2}; \end{aligned} \quad (12)$$

spherical screen: with radius Δ_{GC} centered on Sgr A*:

$$\begin{aligned} \Delta &= \left[\Delta_{\text{GC}}^2 - (D_{\text{GC}} \sin \ell)^2 - (D_{\text{GC}} \sin b)^2 \right]^{1/2} - r \cos \phi, \\ X_s &= \left[\Delta_{\text{GC}}^2 - (D_{\text{GC}} \sin \ell)^2 - (D_{\text{GC}} \sin b)^2 \right]^{1/2}. \end{aligned} \quad (13)$$

In these equations, we consider only the portions of the screens that have $X_s > 0$; i.e., for the cylindrical and spherical screens, we ignore the portions of the screen on the far side of Sgr A*. As we noted earlier, the weighting factor $\Delta_{\text{GC}}/D_{\text{GC}}$ means that the portion of the screen nearest the observer will be the dominant contribution to the scattering. Of course, extragalactic sources would be affected by scattering material on both the near and far side of Sgr A*.

We now transform from Δ to observed scattering diameter, θ_s . For sources behind the screen with separation $\Delta > 0$, the scattering diameter is simply related to that of Sgr A* (θ_{GC}) as

$$\begin{aligned} \theta_s(\Delta) &= \left(\frac{\Delta}{\Delta_{\text{GC}}} \right) \left(\frac{D_{\text{GC}}}{D_{\text{GC}} + \Delta - \Delta_{\text{GC}}} \right) \theta_{\text{GC}} \\ &\approx \left(\frac{\Delta}{\Delta_{\text{GC}}} \right) \theta_{\text{GC}}, \end{aligned} \quad (14)$$

where we consider sources near the GC such that $|\Delta - \Delta_{\text{GC}}| \ll D_{\text{GC}}$. Sources in front of the screen ($\Delta < 0$) are broadened substantially less, in accord with the predictions of the TC93 model, and we therefore assume that the contribution from scattering material in front of the screen is negligible compared with that from the screen. The TC93 scattering diameter is $\theta_s^{(\text{TC})}(\ell, b, D)$ with

$$\begin{aligned} D &= \left[D_{\text{GC}}^2 + (X_s - \Delta)^2 + (D_{\text{GC}} \sin \ell)^2 + (D_{\text{GC}} \sin b)^2 - 2D_{\text{GC}}(X_s - \Delta) \right]^{1/2} \\ &\approx D_{\text{GC}} + \Delta - X_s, \end{aligned} \quad (15)$$

where the approximate equality holds for sources and screen near the GC. We thus have

$$\theta_s = \begin{cases} \theta_{\text{GC}} \left(\frac{\Delta}{\Delta_{\text{GC}}} \right), & \Delta > 0, \text{ behind screen;} \\ \theta_s^{(\text{TC})}(\ell, b, D), & \Delta < 0, \text{ not behind screen.} \end{cases} \quad (16)$$

Transforming from Δ to θ_s , we find

$$f_{\ell, b, \theta_s}(\ell, b, \theta_s) = \begin{cases} \left(\frac{\Delta_{\text{GC}}}{\theta_{\text{GC}}} \right) f_{\ell, b, \Delta}(\ell, b, \Delta = \Delta_{\text{GC}}\theta_s/\theta_{\text{GC}}), & \Delta > 0, \text{ behind screen;} \\ \frac{f_{\ell, b, \Delta}(\ell, b, \Delta \approx D - D_{\text{GC}} + X_s)}{|\partial \theta_s^{(\text{TC})}/\partial \Delta|}, & \Delta < 0, \text{ not behind screen.} \end{cases} \quad (17)$$

From equation (10), the distribution of scattering diameters of OH/IR stars is

$$f_{\ell, b, \theta_s}(\ell, b, \theta_s) = \left(\frac{\Delta_{\text{GC}} D_{\text{GC}}^2}{r \theta_{\text{GC}}} \right) f_{r, \phi, z}(r, \phi, z). \quad (18)$$

For the specific form of equation (8) and a flat scattering screen,

$$\begin{aligned} f_{\ell, b, \theta_s}(\ell, b, \theta_s) &= \\ \left(\frac{\eta \Delta_{\text{GC}} D_{\text{GC}}^2}{\theta_{\text{GC}} a_r^2 a_z} \right) &\left\{ 1 + a_r^{-2} \left[\Delta_{\text{GC}}^2 \left(1 - \frac{\theta_s}{\theta_{\text{GC}}} \right)^2 + (\ell D_{\text{GC}})^2 \right] + \left(\frac{b D_{\text{GC}}}{a_z} \right)^2 \right\}^{-1}. \end{aligned} \quad (19)$$

To form the likelihood, \mathcal{L}_{OH} , we note that equation (19) applies only to sources that are behind the screen. Assume that the screen boundaries transverse to the line of sight are defined by some boundary function, $\mathcal{B}(\ell, b)$. Sources at ℓ, b such that they are not seen through the screen will have scattering angles given by the TC93 model, $\theta_s^{(\text{TC})}(\ell, b)$, that are much smaller than those given by equation (15). In addition, there is measurement error on the scattering diameter whose probability distribution function is a gaussian with standard deviation σ_θ and mean θ_s . This pdf should be convolved with the pdf f_{ℓ, b, θ_s} given above. In all cases we will consider, the width of f_{ℓ, b, θ_s} as a function of θ_s is much wider than the error on θ_s , so that we will use simply equation (19).

The form of equation (19) indicates, for $\Delta_{\text{GC}} \gg a_r$, that the likelihood of a measurement is small unless the scattering diameter is close to that of Sgr A*, $\theta_s \approx \theta_{\text{GC}}$. The sources measured by Frail et al. (1994) satisfy this constraint. The pdf also falls off in ℓ, b if the transverse distances from the GC, ℓD_{GC} and $b D_{\text{GC}}$, are much larger than the respective scales, a_r and a_z . Since highly scattered masers are seen at least 15' from Sgr A* (in the longitude direction), this suggests that a_r is not significantly smaller than $D_{\text{GC}} \times 15 \text{ arc min} \sim 40 \text{ pc}$. This suggests, roughly, that $\Delta_{\text{GC}} \gtrsim a_r \geq 20 \text{ pc}$. Lindqvist et al. (1992) find $a_r \approx 50 \text{ pc}$ and $a_z \approx 35 \text{ pc}$.

The likelihood factor for N_{OH} sources is then

$$\mathcal{L}_{\text{OH}} = \prod_{j=1}^{N_{\text{OH}}} f_{\ell, b, \theta_s}(\ell_j, b_j, \theta_{s,j}). \quad (20)$$

3.1.3. Results

Figure 4 shows the angular broadening likelihood as a function of Δ_{GC} and ψ_ℓ . As a function of ψ_ℓ , this likelihood is constructed by varying ψ_ℓ and using only those OH masers for which $|\ell| < \psi_\ell$. The likelihood function is insensitive to $\psi_b < 1^\circ$; allowing $\psi_b > 1^\circ$ results in OH masers with large latitudes but small longitudes to contribute to the likelihood function. We set $\psi_b = 0.5^\circ$.

As a function of Δ_{GC} , $\mathcal{L}_{\text{broaden}} = \mathcal{L}_{\text{OH}}$ shows a pronounced peak at $\Delta_{\text{GC}} \approx 150 \text{ pc}$. This result is not contrary to our earlier claim in §1 that Galactic sources cannot constrain Δ_{GC} . Any *given* Galactic source cannot constrain Δ_{GC} , because one can adjust SM_s and Δ_{GC} in equation (6) to produce any desired level of angular broadening. However, the OH masers are drawn from a Galactic population whose spatial distribution is known.

Equation (19) implies that \mathcal{L}_{OH} has a maximum as a function of Δ_{GC} . Consider a maser seen through the scattering region, with a measured angular diameter, θ_s , and position (ℓ, b) . The likelihood for this one source is a function of only (Δ_{GC}/a_r) . For small (Δ_{GC}/a_r) , f is approximately linear. However, for large (Δ_{GC}/a_r) , $f \propto (\Delta_{\text{GC}}/a_r)^{-2}$. The combination leads to a peak at $(\Delta_{\text{GC}}/a_r) \sim 1$.

In combination with angular broadening measurements for other sources, the angular broadening likelihood function can also be used to constrain the angular extent of the scattering region. We have evaluated \mathcal{L}_{OH} as a function of ψ_ℓ and ψ_b , with $\Delta_{\text{GC}} = 150 \text{ pc}$. The likelihood is dominated by the masers OH 359.517+0.001, OH 359.581−0.240, and OH 1.369+1.003. We constrain ψ_ℓ to $\psi_\ell \lesssim 45'$; there is no evidence for an asymmetric distribution in ℓ of scattering. The maser OH 359.517+0.001 is nearly 0.5° from Sgr A* in longitude, yet has a diameter 1.5 times larger than that of Sgr A*. The extragalactic source B1739−298 ($\ell = 358.918$, $b = 0.073$) is approximately 1° from Sgr A*, yet has an angular diameter smaller than that of Sgr A* (Paper I). The screen model of Fig. 2 cannot accommodate extragalactic source diameters smaller than that of Sgr A*. Thus, the angular extent of the scattering region to negative longitudes must be $-0.5^\circ > \psi_\ell \gtrsim -1^\circ$. Toward

positive longitudes there are fewer extremely heavily scattered masers. A more severe constraint on the angular extent is provided by H₂O masers and the extragalactic source GPSR 0.539+0.263. In Sgr B ($\approx 45'$ from Sgr A*) H₂O masers have diameters nearly five times smaller than that of Sgr A*, indicating that either they are not behind the extreme scattering region or that they are close to the screen, i.e., have a small Δ . The upper limit on the diameter of the extragalactic source GPSR 0.539+0.263 requires either $\psi_\ell \lesssim 40'$ or that $\Delta_{\text{GC}} \gtrsim 3$ kpc. Given our constraints on Δ_{GC} from above, the lack of scattering for the H₂O masers and GPSR 0.539+0.263 is most likely due to the limited extent of the scattering region. However, a larger angular extent for the scattering region is possible if the scattering screen is patchy.

The angular extent in latitude of the scattering region is less constrained. The maser OH 359.581–0.240 is 0°24 from Sgr A* and has a diameter 30% larger than Sgr A*; OH 1.369+1.003 is 1° from Sgr A* with a diameter only 25% that of Sgr A*. They constrain $\psi_b \lesssim 1^\circ$, but determination of angular diameters for masers (or other sources) within the longitude range $0.25^\circ \lesssim |b| \lesssim 1^\circ$ could provide much more stringent limits.

3.2. Source Counts

Both our observations (Paper I) and those in the CPS show an apparent deficit of sources near Sgr A*. Here we quantify the likelihood that this paucity arises from scattering so severe that extragalactic sources have been resolved out.

3.2.1. Data

Paper I reports a VLA survey of the inner 2° of the GC designed to identify potential extragalactic sources. We observed ten fields at 1.28 and 1.66 GHz; the fields include one or more sources judged likely to be extragalactic on the basis of morphology, spectral information, or both. We also had observations at 5 GHz, but we focus on the 1.28 and 1.66 GHz observations because the 5 GHz observations have smaller fields (a factor ~ 4 in area), so they contain fewer sources, and the scattering diameter is no more than 10'', so that scattering does not desensitize VLA surveys. The observations were conducted in spectral-line mode. As a result a large field of view was obtained and we were able to detect well over 100 sources. We do not detect scatter broadening for any of these sources.

Table 2 shows the number of sources detected in each field. We report the number of Galactic, extragalactic, and unidentified sources; anticipating the results of the next section, we also report the number of extragalactic sources expected.

Differences in the number of sources at the two frequencies detected in the same field arise from three effects in our survey. A trivial, but by far dominant, cause is the smaller field of view

at 1.66 GHz. A second, competing effect is that, in general, the rms noise in the 1.66 GHz images is slightly lower than that for the 1.28 GHz images. Finally, the spectral index of a source could result in it being detectable at only one frequency (a spectral index of 2 results in a factor of 1.6 in the flux between the two frequencies).

In many cases in which a source was detected initially at only one frequency, we have identified a possible counterpart at the other frequency. For the purposes of counting sources, however, we do not consider these possible counterparts to contribute to the total number of sources in the field, at the *other* frequency. For the sake of specificity, we take the example of a source identified at 1.66 GHz and a possible counterpart at 1.28 GHz. This source would contribute only to the 1.66 GHz counts. Our justification for excluding the counterpart from the source counts at 1.28 GHz is that other sources with a similar flux were not equally likely to have been identified. If all sources at 1.28 GHz with a flux comparable to that of the counterpart were equally likely to have been detected, we could describe the survey as being incomplete at a certain level at this flux. This is clearly not the case and we have therefore excluded counterparts from source counts.

3.2.2. Likelihood factor $\mathcal{L}_{\text{counts}}$

Within the fields observed, we detected between 2 and 20 sources per field. We have identified approximately 10% of these sources as either Galactic or extragalactic. The remaining sources are potentially from both Galactic and extragalactic populations. We compare the actual number of sources found in a field, N , to the number expected, $\langle N \rangle$, using a likelihood function

$$\mathcal{L}_{\text{counts}} \equiv \mathcal{L}(N|\theta_{\text{OH}}; \Delta_{\text{GC}}, \psi_{\ell}, \psi_b) = \frac{\langle N \rangle^N}{N!} e^{-\langle N \rangle}. \quad (21)$$

The conditional nature of this likelihood function is apparent from equation (3): The expected number of sources will depend, in part, upon the expected scattering diameter for extragalactic sources given the observed scattering diameters of Galactic sources (i.e., OH masers and Sgr A*).

We shall consider a number of different determinations of $\mathcal{L}_{\text{counts}}$, which differ in the way that we treat the expected number of Galactic sources. We discuss first the contribution of extragalactic sources, $\langle N_{\text{xgal}} \rangle$, and then describe the various methods we have used to estimate the Galactic source contribution.

Extragalactic Sources Within a field of radius Φ , the expected number of extragalactic sources is

$$\langle N_{\text{xgal}} \rangle = \int_0^\Phi d\phi 2\pi\phi \int_{S_{\text{min}}}^\infty \int_0^{\theta_{\text{max}}} dS d\theta \frac{d^2n}{dS d\theta}. \quad (22)$$

Here $d^2n/dS d\theta$ is the areal density of sources on the sky per unit flux density per unit *intrinsic* diameter θ . The limits S_{min} and θ_{max} on the inner integrals result from the *brightness-limited* nature of VLA surveys: A source must be both sufficiently strong ($\geq S_{\text{min}}$) and compact ($\leq \theta_{\text{max}}$)

to be detected. These limits are not constant, but, for clarity, we have suppressed the functional dependences in equation (22).

We have searched for and detected sources at considerable distances from the field (phase) center, $\Phi \geq 20'$. Due to the VLA's primary beam attenuation, the minimum detectable flux density for a point source increases with distance from the phase center, $S_{\min} = S_{\min}(\phi)$. At the phase centers of the various fields, $S_{\min}(0)$ is 2 to 8 mJy (Paper I).

The maximum diameter for a detectable source, θ_{\max} , depends upon VLA configuration, flux density, and scattering diameter:

VLA configuration: The largest angular structure which can be detected by the VLA depends upon the length of the shortest baselines. For our program, the VLA was in the BnA configuration (Paper I). Combined with the snapshot mode of observation, the largest detectable source diameters are approximately $60''$; for some fields near Sgr A*, we imposed additional u - v constraints that reduced this limit to $30''$.

Flux density: Extragalactic sources show a distribution of intrinsic angular diameter that depends on S . Even in the absence of scattering, some sources are extended enough to escape detection, either because the source is below our minimum detectable brightness or because the VLA configuration is not sensitive to the source. The fraction of sources intrinsically large enough to avoid detection is not negligible in the flux density range of interest. For instance, at 10 mJy, approximately 10% of all sources have diameters larger than $30''$ (Windhorst, Mathis, & Neuschaefer 1990).

Scattering diameter: Larger scattering diameter, θ_{xgal} , diminishes the detectability of sources, either by making sources fall below our minimum detectable brightness or by decreasing the fraction of sources to which the VLA configuration is sensitive.

We define the fraction of sources compact enough to be detected in our program as

$$f_{<}(\theta_{\max}|S; \theta_{\text{xgal}}; \text{VLA}) = \frac{\int_0^{\theta_{\max}} d\theta d^2n/dS d\theta}{\int_0^{\infty} d\theta d^2n/dS d\theta}. \quad (23)$$

The quantity θ_{\max} is the largest *intrinsic* diameter that can be detected. The minimum detectable brightness at constant S depends upon the maximum *apparent* diameter, $I_{\min} \propto S/\theta_{\text{app,max}}^2$. We take the intrinsic and scattering diameters to add in quadrature to produce the apparent diameter, $\theta_{\text{app,max}}^2 = \theta_{\max}^2 + \theta_{\text{xgal}}^2$. We also define the areal density of sources of all intrinsic diameters per unit flux density as

$$\frac{dn}{dS} = \int_0^{\infty} d\theta \frac{d^2n}{dS d\theta}. \quad (24)$$

This quantity is reported commonly in log N -log S measurements.

The expected number of extragalactic sources is then

$$\langle N_{\text{xgal}} \rangle = \int_0^\Phi d\phi 2\pi\phi \int_{S_{\min}(\phi)}^\infty dS f_<(\theta_{\max}|S; \theta_{\text{xgal}}; \text{VLA}) \frac{dn}{dS}. \quad (25)$$

In evaluating $\langle N_{\text{xgal}} \rangle$ we use the description of the primary beam from the AIPS task **PBCOR** for $S_{\min}(\phi)$ and equation (3) to calculate θ_{xgal} . We use Katgert, Oort, & Windhorst's (1988) fit to 1.4 GHz source counts for dn/dS , and for $f_<$ we use the intrinsic diameter distribution of Windhorst et al. (1990). A more recent assessment (the FIRST survey) of both $f_<$ and dn/dS shows excellent agreement between the functional forms we have adopted and the distributions inferred from over 10^5 sources (White et al. 1997).

We close with a caveat. Equation (3) for θ_{xgal} assumes a single scattering screen. If the scattering material wraps around the GC, cf. Fig. 1, forming an effective screen on both the near and far sides of the GC, the actual scattering diameters would be at least a factor of two larger. If the scattering region fills the GC, the scattering could be even larger. A larger θ_{xgal} than we assume results in less stringent constraints on Δ_{GC} .

Galactic Sources The second contribution to $\langle N \rangle$ is from Galactic sources. We consider three methods for estimating the Galactic source contribution, $\langle N_{\text{Gal}} \rangle$:

1. Assume that no Galactic sources are present;
2. Use the Galactic source distribution inferred from the CPS (Helfand et al. 1992; Becker et al. 1994); and
3. Estimate the Galactic source distribution from the fields in our survey.

The Galactic radio source population is dominated by H II regions (Becker et al. 1992). There are localized regions of enhanced star formation within the GC, e.g., Sgr B, but the star formation rate of the inner 100 pc or so is $\lesssim 10\%$ of the Galactic rate (Güsten 1989), and, in general, the inner 100 pc is not the site of current, vigorous massive star formation (Morris & Serabyn 1996). Thus, although Method 1 will underestimate the Galactic population toward star forming regions, on average it should not be too severe of an underestimate of the Galactic contribution to GC fields. The utility of Method 1 is that it produces a minimal estimate of $\langle N \rangle$. Method 1 therefore places an upper limit on the strength of scattering for fields with a deficit of sources.

Extended sources (diameters $> 3''$) in the CPS are concentrated toward both the inner Galaxy and the Galactic plane. Becker et al. (1992) identify these sources with a population of extreme Population I objects (largely compact and ultra-compact [UC] H II regions) having flux densities $S \geq 25$ mJy. Toward the inner Galaxy, $-20^\circ \leq \ell \leq 40^\circ$, the areal density of these sources is

$$n_{\text{Gal}}^{(2)} \approx 7.5 \text{ deg}^{-2} \exp \left[-(b/0^\circ 3)^2 \right]. \quad (26)$$

Any other population of Galactic radio sources must have a scale height larger than approximately 2° (Helfand et al. 1992). Thus, the number of Galactic sources can be estimated from the area of the field of view ($\sim 1 \text{ deg}^2$) and equation (26). This concentration of UCH II regions to the inner Galaxy does not contradict our assumption of Method 1 because of the different regions involved. The concentration toward the inner Galaxy occurs over tens of degrees while the GC is only 1° in size.

While Method 2 allows N_{Gal} to be estimated, it does require certain caveats. First, unlike extragalactic sources, these Galactic sources are unlikely to be distributed randomly. UCH II regions are often observed to be clustered within their natal molecular clouds (Churchwell 1990). Thus, the areal density of equation (26) will likely underestimate the number of sources in fields containing star forming regions, while overestimating the number for fields lacking from star forming regions. Second, the conditions for star formation in the GC are suitably different from those in the disk (Morris & Serabyn 1996) that it may not be valid to extend equation (26) to fields within the GC.

A visual comparison shows that the fields in our survey with $|b| \approx 1^\circ$ appear to contain fewer sources than those near $b = 0^\circ$ (Paper I). We have assumed the high latitude fields ($|b| > 1^\circ$) contain only extragalactic sources while the low latitude fields ($|b| < 1^\circ$) contain a mixture of extragalactic and Galactic sources. We have taken the Galactic sources to have a gaussian distribution in latitude and used a maximum likelihood method to solve for the amplitude and width of this distribution. Using the source counts at 1.28 GHz for those fields more than 1° from Sgr A*, we find

$$n_{\text{Gal}}^{(3)} \approx 8.9 \text{ deg}^{-2} \exp \left[-(b/0^\circ 3)^2 \right]; \quad (27)$$

a similar amplitude with a slightly larger width ($0^\circ 4$) results if we use the source counts from 1.66 GHz.

Method 3 determines n_{Gal} from our own data within the region of interest, the inner few degrees, in contrast to Method 2, which is derived from most of the inner Galaxy. Method 3 should be less susceptible to variations between the GC and other regions of the Galaxy, though variations within the GC will still be important.

3.2.3. Results

We evaluate the likelihoods for the individual fields, equation (21), assuming that the likelihoods are a function of Δ_{GC} only. The sizes of these fields are comparable to the known angular extent of the scattering region. Rather than attempt to detect changes in the number of sources as a function of position within a field, we simply assume that a field is covered entirely by the scattering region and compute the expected number of sources within the field as a function of Δ_{GC} .

We shall obtain information about the angular extent of the scattering region in the following

manner. We assume that the scattering diameter of a Galactic source is that of Sgr A*, regardless of the angular distance of the field from Sgr A*. Since OH masers near Sgr A* have diameters comparable to that of Sgr A*, the scattering diameter of Sgr A* is a reasonable description of the level of scattering, and the expected number of sources should be roughly equal to the observed number of sources, i.e., the likelihood should be near unity. At large distances from Sgr A*, the scattering diameter of Sgr A* (presumably) overestimates the level of scattering, and the expected number of sources will be considerably less than the observed number, i.e., the likelihood should be considerably less than unity. By determining at what angular distance the expected number of sources becomes significantly less than the observed number, we can place crude limits on the angular extent of the scattering region.

Figure 5 displays the likelihoods for three fields, $359.9+0.2$, $358.9+0.5$, and $358.1-0.0$. These fields range from $15'$ to 2° from Sgr A* and exemplify results for fields at small, intermediate, and large distances from Sgr A*, respectively. For the fields $358.9+0.5$ and $358.1-0.0$ we show the Method 3 likelihoods in which the number of Galactic sources is estimated from our observations. The other methods described in §3.2.2 produce likelihoods with similar shapes—the amplitudes for Method 2 are similar; for Method 1 the amplitudes are lower. For the field $359.9+0.2$ we show both the Method 1 and 3 likelihoods, the Method 2 likelihood is similar to the Method 3 likelihood.

The likelihood for $358.1-0.0$, the field farthest from Sgr A*, shows a minimum at small Δ_{GC} , increasing with increasing Δ_{GC} . If Δ_{GC} is small, this field has an excess of sources relative to what one expects given the large scattering diameter. For larger Δ_{GC} , fewer sources are expected to be resolved out and the likelihood increases. The likelihood for field $358.9+0.5$, at an intermediate distance from Sgr A*, has a similar shape, though the minimum of the likelihood is not as pronounced, indicating that the excess is not as severe. Finally, the likelihood for $359.9+0.2$, the field closest to Sgr A*, shows the exact opposite shape. The likelihood is a maximum at small Δ_{GC} , decreasing toward larger Δ_{GC} . This decrease reflects the increasing number of extragalactic sources expected as Δ_{GC} increases and fewer sources are expected to be resolved out. Thus, these likelihood functions are consistent with the GC model, a scattering region local to the GC. The half-power point for the likelihood occurs at $\Delta_{\text{GC}} \approx 500$ pc. The Method 1 likelihood, which compares only the number of extragalactic and unidentified sources to the expected number of extragalactic sources, has a maximum at intermediate Δ_{GC} . At small Δ_{GC} , there is an excess of sources, because we find one source but expect none due to the extreme broadening. At large Δ_{GC} there is a deficiency of sources as scattering is no longer severe enough to resolve out many sources. At intermediate Δ_{GC} , $200\text{ pc} \lesssim \Delta_{\text{GC}} \lesssim 700\text{ pc}$, the scattering is such that most, but not all, extragalactic sources are expected to be resolved out.

In fact, it is likely that $\Delta_{\text{GC}} < 200$ pc. There are no extragalactic sources in the field $359.9+0.2$ and only one unidentified source, 1LC $359.873+0.179$. We list this source as unidentified because its morphology is suggestive of an extragalactic source yet it does not show the level of scattering expected for an extragalactic source seen through the entire Galactic disk (Paper I). If we exclude this source from the calculation of the Method 1 likelihood, i.e., take the source to be Galactic, the

paucity of sources in this field requires $\Delta_{\text{GC}} < 200$ pc.

We have performed a similar analysis for the fields from the CPS. We find the same general pattern for their fields as for ours. Fields far from Sgr A*, particularly those at latitudes $|b| > 0^\circ.5$, show likelihood minima at small Δ_{GC} . Fields approximately 1° from Sgr A*, particularly those at $b = 0^\circ$, show a nearly constant likelihood. Fields within 1° of Sgr A* show likelihood maxima at small Δ_{GC} . Because of the smaller fields ($\Phi = 15'$) and generally larger $S_{\min}(0)$ for the CPS fields, fewer extragalactic sources are expected and the derived constraints on Δ_{GC} are weaker than those from our fields.

Figure 6 shows the combined source count likelihood as a function of Δ_{GC} and ψ_ℓ , the angular extent of the scattering screen in longitude. We construct this likelihood function by multiplying the likelihood functions for those fields with $|\ell| < \psi_\ell$. We focus on ψ_ℓ as a measure of the angular extent of the screen because our fields (and the OH/IR stars) are displaced from Sgr A* primarily in longitude. We fix $\psi_b = 0^\circ.5$. The likelihood function is insensitive to the choice of ψ_b for $\psi_b \lesssim 1^\circ$; for $\psi_b > 1^\circ$ the likelihood function is altered by fields with small longitudes, but large latitudes. The figure reflects the conclusions we have already drawn from examining only three fields. Over the region $\Delta_{\text{GC}} \lesssim 500$ pc and $\psi_\ell \lesssim 1^\circ$, the likelihood is maximized and roughly constant.

Even though we display $\mathcal{L}_{\text{counts}}$ for ψ_ℓ as large as 2° , $\psi_\ell > 1^\circ$ is unlikely. As discussed in §3.1.3, the angular broadening of various extragalactic sources and H₂O masers constrains the angular extent of the region to be less than 1° .

Two effects could make the limits on Δ_{GC} less stringent. First, as noted in the previous section, we calculate θ_{xgal} using equation (3) which assumes a single screen. If the scattering material wraps around the GC, so that there is a near and far side screen, the actual scattering diameters will be at least a factor of two larger than those calculated here.

Second, the above results assume the nominal vignetting correction contained in the task **PBCOR**. Zoonematkermani et al. (1990) suggested that **PBCOR** undercorrects flux densities at large distances ($\Phi > 20'$) from the phase center. If the flux densities at large distances from the phase center are undercorrected, the limit $S_{\min}(\phi)$ on the integral over S in equation (22) will be too small. Consequently, the estimate of $\langle N_{\text{xgal}} \rangle$ will be too large.

The primary beam correction factor is a function of both distance from the phase center and observing frequency. By comparing the corrected flux densities of sources observed in multiple fields, i.e., at multiple distances from phase centers, Zoonematkermani et al. (1990) arrived at better estimates for the primary beam correction factor if they adopted an effective frequency which was larger than their observing frequency by about 0.2 GHz. We repeated the above analysis for the field 359.9+0.2 at 1.28 GHz, adopting an effective frequency of 1.4 GHz. We find a similar shape for the likelihood function, though the upper limit on Δ_{GC} is less stringent, $\Delta_{\text{GC}} \lesssim 0.7\text{--}1$ kpc.

3.3. Free-Free Emission and Absorption Measurements

As described in §2, the density fluctuations responsible for scattering should also contribute to the emission measure and therefore to free-free emission and absorption. In this section we use angular broadening measurements to estimate EM_{SM} and from this, the free-free intensity, I_{SM} , and optical depth, τ_{SM} . We then compare these values to those derived from measurements, I_{ff} and τ_{ff} .

3.3.1. Data

We shall focus on five masers from the Frail et al. (1994) results in order to predict EM_{SM} . These masers are listed in Table 3. All have angular diameters (or geometric means of their major and minor axes) greater than that of Sgr A*, all but one show elliptical scattering disks, and all are $\geq 15'$ from Sgr A*. As the free-free emission is highly concentrated toward Sgr A*, these masers provide the most stringent constraints on the amount of emission contributed by the density fluctuations responsible for scattering. Our use of these scattering diameters in determining EM is the reason that the likelihood function we derive will be a *conditional* likelihood.

We estimate the free-free emission along the line of sight to these masers from the 10 GHz survey of Handa et al. (1987). We apply two corrections to the observed brightness temperature along these lines of sight. First, the GC contains both thermal and non-thermal radiation. Mezger & Pauls (1979) report on multi-frequency observations, at $\nu \leq 5$ GHz, from which the GC emission is decomposed into thermal and non-thermal components. From those results, approximately 60% of the 10 GHz emission is thermal. The second correction is that the density fluctuations responsible for angular broadening are bounded by $\delta n_e \leq \bar{n}_e$. Hence, at most, only half of the thermal emission along the line of sight to the GC can occur within the scattering region. In summary, of the total emission in the direction of the GC, at most 30% of it can be attributed to the density fluctuations in the scattering region.

We estimate the free-free absorption from the 0.327 GHz observations of Anantharamaiah et al. (1991). Over the northern section of the Arc, they estimated $\tau_{\text{ff}} \approx 1$. The fact that they detected the Arc and Sgr C, both at distances from Sgr A* comparable to some of the heavily scattered OH masers, indicates that τ_{ff} cannot be much larger than unity (see Fig. 2 of Frail et al. 1994). At 0.16 GHz, many of the GC features cannot be detected, indicating that $\tau_{\text{ff}} > 1$ at this frequency (Yusef-Zadeh et al. 1986). Earlier attempts to constrain the scattering toward the GC have focussed on the absorption toward Sgr A* only (e.g., van Langevelde et al. 1992). Sgr A* becomes obscured near 1 GHz (Davies et al. 1976a; but see also Beckert et al. 1996). However, Sgr A* is embedded in the Sgr A West H II region (Pedlar et al. 1989; Anantharamaiah et al. 1991) and additional absorption may be contributed by this gas. Any additional, absorbing gas within Sgr A West would contribute little to the scattering of Sgr A* due to the weighting $(R_c/D_{\text{GC}})^2$ in equation (6). As for the thermal emission, the density fluctuations only contribute to half the total

free-free optical depth, $\tau_{\text{SM}} \leq \tau_{\text{ff}}/2$.

3.3.2. Likelihood factor \mathcal{L}_{ff}

The EM corresponding to a source of diameter θ_s is (van Langevelde et al. 1992)

$$\text{EM} = 10^{2.74} \text{ pc cm}^{-6} \left(\frac{l_0}{1 \text{ pc}} \right)^{2/3} \left(\frac{l_1}{100 \text{ km}} \right)^{1/3} \left(\frac{D_{\text{GC}}}{\Delta_{\text{GC}}} \right)^2 \left(\frac{\theta_s}{133 \text{ mas}} \right)^2. \quad (28)$$

Although the EM does depend on the inner scale, l_1 , this dependence is weak compared to the other dependences in equation (28). Henceforth, we will assume $l_1 = 100 \text{ km}$.

Our initial attempts to form the free-free likelihood also included the free-free absorption. However, we found that the likelihood was dominated by the contribution from T_{ff} , reflecting the fact that we have only upper limits on the free-free absorption. Henceforth, we shall restrict our attention to only the free-free emission. The adopted likelihood function is

$$\mathcal{L}_{\text{ff}} = \mathcal{L}(T_{\text{ff}} | \theta_{\text{OH}}, N; \Delta_{\text{GC}}, \psi_\ell, \psi_b, l_0, T_e) = \prod_{j=1}^N \exp \left[- (T_{\text{ff},j} - T_{\text{SM},j})^2 / 2\delta T_{\text{ff},j}^2 \right]. \quad (29)$$

Here T_{SM} is the emission predicted from the angular broadening measurements and T_{ff} is the measured quantity (with the corrections described above). We use the brightness temperature as a measure of the free-free emission because that is the quantity reported by Handa et al. (1987). In addition to the dependence on l_0 and Δ_{GC} , T_{SM} also depends on the electron temperature T_e .

Our estimate for δT_{ff} reflects how accurately we can register the maser positions in the 10 GHz survey (Handa et al. 1987) and the spacing between contours. We adopt $\delta T_{\text{ff}} = 0.5 \text{ K}$, corresponding to $\delta T_{\text{ff}}/T_{\text{ff}} \approx 0.1$ to 0.5.

The predicted intensity is

$$T_{\text{SM}} \propto l_0^{2/3} T_e^{-1/2} \Delta_{\text{GC}}^{-2}, \quad (30)$$

where we have ignored the logarithmic dependence on temperature in the Gaunt factor. In contrast to the previous likelihoods in which Δ_{GC} was orthogonal to the other parameters, the free-free likelihood cannot constrain Δ_{GC} independently of l_0 and T_e .

3.3.3. Results

Figure 7 shows \mathcal{L}_{ff} as a function of Δ_{GC} and $l_0^{2/3} T_e^{-1/2}$, with l_0 in parsecs and T_e in K. As expected from equation (30), the maximum likelihood occurs on a line of constant $l_0^{2/3} T_e^{-1/2} \Delta_{\text{GC}}^{-2}$. The corrections we have applied to the measured brightness temperatures shift the region of maximum likelihood to the left, i.e., to smaller $l_0^{2/3} T_e^{-1/2}$ at constant Δ_{GC} .

The absence of free-free absorption toward Sgr A* at frequencies above 1 GHz constrains $\Delta_{\text{GC}}/D_{\text{GC}}$ to be $0.1 \leq \Delta_{\text{GC}}/D_{\text{GC}} \leq 0.32$, for nominal values of $l_0 = 1$ pc and $T_{\text{e}} = 10^4$ K (van Langevelde et al. 1992). The upper and lower limits scale as $l_0^{1/3} T_{\text{e}}^{-0.675}$. If these nominal values are correct, the free-free emission likelihood of Fig. 7 indicates that $\Delta_{\text{GC}}/D_{\text{GC}}$ would exceed unity. Since the other two likelihoods are maximum for $\Delta_{\text{GC}}/D_{\text{GC}} < 0.1$, we anticipate that the scattering region has $l_0 < 1$ pc, $T_{\text{e}} > 10^4$ K, or both. We defer estimates of l_0 and T_{e} until we have formed the global likelihood in the following section.

In forming this likelihood function we have assumed that all five of the masers in Table 3 are affected by the scattering screen. The free-free likelihood does not constrain the angular extent of the screen except that we have assumed the screen covers all of the masers used. The angular extent of the screen is therefore at least $25'$.

3.4. Global Likelihood for Galactic Center Scattering

Figures 4, 6, and 7 show the individual likelihoods, $\mathcal{L}_{\text{counts}}$, $\mathcal{L}_{\text{broaden}}$, and \mathcal{L}_{ff} , respectively. We now combine these to form the global likelihood, \mathcal{L} , equation (7). This global likelihood has four parameters, Δ_{GC} , ψ_{ℓ} , ψ_b , and $l_0^{2/3} T_{\text{e}}^{-1/2}$. Because ψ_b is poorly constrained (§3.1.3), we shall hold it fixed at $\psi_b = 0^\circ.5$.

Figure 8 shows \mathcal{L} projected onto the $\Delta_{\text{GC}}\text{-}\psi_{\ell}$ and $\Delta_{\text{GC}}\text{-}(l_0^{2/3} T_{\text{e}}^{-1/2})$ planes. As a function of Δ_{GC} and ψ_{ℓ} , the maximum likelihood occurs at $\Delta_{\text{GC}} = 133_{-80}^{+200}$ pc and over the range $0.5^\circ \leq \psi_{\ell} \leq 1.2^\circ$. The ranges for these parameters enclose the 90% confidence region and are obtained by marginalizing the global likelihood; henceforth we adopt $\Delta_{\text{GC}} = 150$ pc. The maximum likelihood estimate for Δ_{GC} is determined primarily by the $\mathcal{L}_{\text{broaden}}$ factor. $\mathcal{L}_{\text{counts}}$ is constant for $\Delta_{\text{GC}} \lesssim 500$ pc while \mathcal{L}_{ff} cannot constrain Δ_{GC} . The angular extent of the scattering region is determined by the combination of $\mathcal{L}_{\text{counts}}$ and $\mathcal{L}_{\text{broaden}}$. The maximum likelihood estimate for the angular extent is consistent with the discussion in §3.1.3, where we used individual lines of sight.

At the distance of the GC, 150 pc $\approx 1^\circ$. This close correspondence between the radial and transverse sizes of the scattering region, as given by the values of Δ_{GC} and $\psi_{\ell} D_{\text{GC}}$, indicates that the scattering region probably encloses or fills the entire GC, rather than being a simple screen as we have assumed, cf. Fig. 1.

With our maximum likelihood estimate of Δ_{GC} , we predict that the scattering diameter for a background source seen through the GC is $90''$, if the scattering is in the form of a single screen, or $180''$, if the scattering region encloses the GC, as appears probable. This large scattering diameter makes the GC the most extreme site of scattering known in the Galaxy; the second strongest scattering region in the Galaxy is the H II complex NGC 6634, which produces a scattering angle of nearly $7''$ at 1 GHz (Moran et al. 1990). The large scattering diameter is almost certainly a reflection of the unique conditions in the GC.

As a function of Δ_{GC} and $l_0^{2/3}T_{\text{e}}^{-1/2}$, the likelihood has a single maximum at the same Δ_{GC} as above and $\log l_0^{2/3}T_{\text{e}}^{-1/2} = -7.0 \pm 0.8$. If $T_{\text{e}} = 10^4$ K, then $l_0 = 10^{-7.5}$ pc; if $l_0 = 1$ pc, then formally $T_{\text{e}} = 10^{14}$ K. The value of $l_0^{2/3}T_{\text{e}}^{-1/2}$ in the GC is smaller than that in the solar neighborhood, $l_0^{2/3}T_{\text{e}}^{-1/2} \sim 10^{-2}$, i.e., $l_0 = 1$ pc and $T_{\text{e}} = 10^4$ K (Rickett 1990; Spangler 1991; Armstrong et al. 1995; and references within). However, there is a small body of evidence that indicates heavily scattered lines of sight have $l_0 \lesssim 10^{-2}$ pc (Frail, Kulkarni, & Vasisht 1993) and Backer (1978) used the scattering of Sgr A* alone to determine that a characteristic size scale for the turbulence is approximately 5 km. If we do not apply the corrections described in §3.3.1, the maximum likelihood estimate of $l_0^{2/3}T_{\text{e}}^{-1/2}$ increases by about an order of magnitude. In §4.2, we consider host media for the scattering region in light of our constraint on $l_0^{2/3}T_{\text{e}}^{-1/2}$.

4. Discussion and Conclusions

4.1. Comparison with Previous Analyses

Isaacman (1981) surveyed the central $2^\circ \times 4^\circ$ ($\ell \times b$) of the GC in a search for planetary nebulae. He finds an *excess* number of sources as compared to that expected from extragalactic source counts, an excess he attributes to H II regions and planetary nebulae. That he finds an excess at all is notable, though, since our analysis predicts that angular diameters of extragalactic sources seen through the GC scattering region will be at least $1.5' - 3'$. The resolution of his survey was $0.4' \times 2'$, and he was able to detect sources with angular scales as large as $14'$. Thus, we attribute his excess to the fact that, where his survey overlapped the GC scattering region, it was desensitized by the intense GC scattering to a considerably lesser degree than our survey.

Anantharamaiah et al. (1991) used their observations at 0.327 GHz and a 0.408 GHz $\log N$ - $\log S$ relation to conclude that the number of observed extragalactic sources within a 4 deg^2 area centered on Sgr A* is consistent with the number expected from high-latitude source counts. Outside of the inner 1 deg^2 , our source counts are also consistent with the expected number of extragalactic sources. Although scattering of other sources, such as B1739–298 and B1741–312 is heavy, the predicted diameter of these sources is less than $10''$ at 0.327 GHz, comparable to the size of their beam, so that these sources would not have been resolved out.

Gray et al. (1993) surveyed the Sgr E region ($\ell = 358.7^\circ, b = 0^\circ$) at 0.843, 1.45, and 4.86 GHz. At 1.4 GHz the number of sources they find is consistent with that expected from the $\log N$ - $\log S$ distribution. Figure 5 shows that the likelihood function for our field $358.9+0.5$ does not favor a large amount of scattering, i.e., the number of sources in this field is consistent with that expected. Further, two of the sources observed in our VLBI experiment (Paper I), B1739–298 and 1LC 358.439–0.211, are in this field. The former is heavily scattered, though not at a level sufficient for it to be seen through the Sgr A* scattering screen.

We conclude that our source count results are in good agreement with previous source counts

toward the GC. The only exception occurs over the 1 deg² region centered on Sgr A*. This region has not been considered previously or has been subsumed into a much larger area.

4.2. Physical Conditions in the Scattering Region

Our global likelihood, Fig. 8 and §3.4, attained a maximum for the following parameter values: $\Delta_{\text{GC}} = 150$ pc, $0.5^\circ \leq \psi_\ell \lesssim 1^\circ$, and $l_0^{2/3} T_e^{-1/2} = 10^{-7}$. In this section we consider whether a medium exists within the GC for which such parameter values are plausible. There is a wealth of observational data available for the GC. We shall summarize those conclusions relevant to our study here; interested readers are referred to a number of recent reviews—Genzel, Hollenbach, & Townes (1994); Morris & Serabyn (1996); and Gredel (1996)—and references within.

Our criteria for the host medium of the density fluctuations are that the medium must have a sufficient density and that it must be capable of sustaining density fluctuations of the requisite magnitude. We establish our first criterion by estimating \bar{n}_e from the scattering diameters of GC sources using equations (5) and (6). The diameters of Sgr A* and the OH masers require a weighted scattering measure of $S \approx 10^2$ kpc m^{-20/3}, equation (6). Eliminating SM between equations (5) and (6) and solving for \bar{n}_e yields

$$\bar{n}_e \sim 10^3 \text{ cm}^{-3} \frac{1}{\varepsilon \sqrt{f}} \left(\frac{l_0}{1 \text{ pc}} \right)^{1/3} \left(\frac{\Delta_{\text{GC}}}{150 \text{ pc}} \right)^{-3/2}. \quad (31)$$

Two factors could alter this estimate by about an order of magnitude. First, it is likely that $l_0 \ll 1$ pc, which would *reduce* our estimate of \bar{n}_e . Second, as we noted in §3.4, the similarity between the values of Δ_{GC} and $\psi_\ell D_{\text{GC}}$ suggests that the density fluctuations fill the region and $f \approx 1$. However, we might also associate l_0 with the characteristic size of a scattering cloudlet within the region. If the region contains few such cloudlets and $\Delta_{\text{GC}}/l_0 \gg 1$, then $f \ll 1$, and our estimate above would be a considerable *underestimate*. Yusef-Zadeh et al. (1994) estimated that a typical line of sight might intersect only 10 or so scattering cloudlets.

In any event, we conclude that the scattering medium must be dense, $n_e \gtrsim 10^2$ cm⁻³. For comparison, Spangler (1991) concludes that $n_e \sim 1$ cm⁻³ for scattering regions in the Galactic disk.

Our second criterion for the host medium is that it must be able to support density fluctuations of the required magnitude. This constraint has been lucidly reviewed by Spangler (1991): The density fluctuations are presumed to arise from plasma turbulence. As this turbulence dissipates, it cannot heat the host medium at a rate that exceeds the medium's cooling capacity. This constraint is particularly acute in the situation we are proposing as the dissipation mechanisms considered by Spangler (1991) scale as l_0^{-a} with $a \approx 1$. Since we are considering $l_0 < 1$ pc, the heating rates could be excessive.

The dominant damping mechanisms for $l_0 < 1$ pc are linear Landau damping, ion-neutral collisions, and a parametric decay instability. The first two mechanisms scale as $l_0^{-2/3}$ while

the latter scales as l_0^{-1} . In addition to their dependence on l_0 , the damping rates depend on the large scale magnetic field, $\Gamma \propto B^2$; the Alfvén wave speed, v_A ; and the amplitude of the magnetic fluctuations, $\Gamma \propto (\delta B/B)^2$ for linear Landau damping and ion-neutral collisions while $\Gamma \propto (\delta B/B)^3$ for the parametric decay instability. Linear Landau damping also depends upon the angle of propagation with respect to the direction of \mathbf{B} , χ , and the plasma β . For values of these quantities appropriate for scattering regions in the Galactic disk, these damping mechanisms produce volumetric heating rates of $\Gamma \sim 10^{-23.5} - 10^{-21.5}$ erg s $^{-1}$ cm $^{-3}$. As Spangler (1991) discussed, there are also a number of simplifications and additional assumptions which enter the calculation of these heating rates.

Inferred magnetic field strengths in the GC are $B \sim 1$ mG, or 10^3 that of the field strength in the disk. To estimate $\delta B/B$, we use (Cordes, Clegg, & Simonetti 1990)

$$\frac{\delta n_e}{n_e} \sim \left(\frac{\delta B}{B} \right)^c \quad (32)$$

with $c = 1$ for linear processes and $c = 2$ for non-linear processes like the parametric decay instability. Our first criterion for the host medium is that $\delta n_e/n_e \leq 1$. For definiteness, and to provide the largest possible value of the heating, we take $\delta B/B \sim 1$. Finally, although B is much larger in the GC than in the Galactic disk, n is also larger. As a result v_A is larger than in the disk, but probably by no more than an order of magnitude. Thus, we expect Γ in the GC to be about a factor of 10^7 larger than in the Galactic disk.

The heating rate from linear Landau damping in scattering regions in the Galactic disk (Spangler 1991) assumes the density fluctuations arise from obliquely propagating magnetosonic waves ($\chi \approx 6^\circ$). More aligned propagation results in less damping. It is not clear if the GC environment would favor highly aligned propagation or not. The large values of B in the GC are inferred, in part, from the system of non-thermal filaments and threads seen throughout the GC. With only one exception, these filaments have no kinks or bends in them, even though they are observed to be interacting with molecular clouds having typical velocities of 10–100 km s $^{-1}$ (Morris & Serabyn 1996). This rigidity could be an indication that only highly aligned propagation is allowed. If χ is highly concentrated near 0° , then the heating from linear Landau damping would be unimportant and the heating rates could be two orders of magnitude lower than those quoted above. Alternately, as Spangler (1991) noted, the distribution of χ could be isotropic, but waves with large χ would then damp quickly and the heating rate will be unchanged or even larger than what we assume.

The presence of small-scale (≈ 0.1 pc) magnetohydrodynamic cloudlets in the GC has already been inferred to explain large changes in the Faraday rotation measure of certain features (G 359.1–00.2, the “Snake,” Gray et al. 1995; G 359.54+0.18, the non-thermal filaments, Yusef-Zadeh, Wardle, & Parastaran 1997), though the inferred density in these cloudlets, 0.3–10 cm $^{-3}$, is less than our nominal estimate. In the Galactic disk a small body of observational evidence suggests that the magnetohydrodynamic medium responsible for Faraday rotation is also responsible for scattering and pulsar dispersion (Simonetti & Cordes 1986; Lazio, Spangler, & Cordes 1990; Minter & Spangler 1996),

and the same may be true in the GC.

We now consider two models for the host medium. In both models, the scattering arises in thin layers on the surfaces of molecular clouds. Even if the filling factor, f , of these layers is not large, the *covering factor*, i.e., the probability that a line of sight through the GC will intersect one of these layers, can still be close to unity.

4.2.1. Photoionized Surfaces of Molecular Clouds

Over the region $|\ell| \lesssim 1^\circ 5$ and $|b| \lesssim 0^\circ 5$, $n_e \sim 10 \text{ cm}^{-3}$, as determined from single-dish recombination line and total intensity measurements (Matthews, Davies, & Pedlar 1973; Mezger & Pauls 1979). Embedded within this large-scale region are smaller regions of much higher electron densities, $n_e \sim 10^3\text{--}10^5 \text{ cm}^{-3}$, primarily within Sgr A West and Sgr B2 (e.g., Mehringer et al. 1993). Some of these high density regions are the photoionized surfaces (size $\sim 10^{-4} \text{ pc}$) of molecular clouds ($n \gtrsim 10^4 \text{ cm}^{-3}$) irradiated by the ambient radiation field (effective temperature $\approx 35\,000 \text{ K}$). Yusef-Zadeh et al. (1994) identified these molecular skins as the source of the scattering and associated their thicknesses with the outer scale, l_0 ; Gray et al. (1995) suggested that the magnetoionic medium responsible for the Faraday rotation toward G 359.1–00.2 also results from these molecular clouds.

This model suffers from at least three potential difficulties. First, the molecular skins are photoionized by a radiation field having a temperature of $T_{\text{eff}} \sim 10^4 \text{ K}$. Our constraint on $l_0^{2/3} T_e^{-1/2}$ therefore requires $l_0 \sim 10^{-7.1} \text{ pc}$. This value is considerably smaller than that derived by Yusef-Zadeh et al. (1994) for the ionized molecular skins. However, in deriving their value for l_0 , Yusef-Zadeh et al. (1994) used a value of the ionizing flux appropriate to the inner few parsecs. The stellar density decreases as r^{-2} , so outside the inner few parsecs, the ionizing flux should be lower than that assumed by Yusef-Zadeh et al. (1994). A lower ionizing flux would result in a smaller skin depth and bring their estimate and our estimate of l_0 into better agreement.

A second potential difficulty with this model is that the medium would only barely be capable of cooling itself. If the outer scale is $l_0 \sim 10^{-7} \text{ pc}$, then the heating rate from the damping of the plasma turbulence is $\Gamma \sim 10^{-13}\text{--}10^{-12} \text{ erg cm}^{-3} \text{ s}^{-1}$. The cooling capacity of gas near $T_e \sim 10^4 \text{ K}$ depends sensitively upon the fractional ionization and temperature (Dalgarno & McCray 1972). We estimate that a density of $n_e \gtrsim 10^5 \text{ cm}^{-3}$ is required for these skins to be able to cool sufficiently in order to support the density fluctuations. This density is at the upper end of the range $10^3\text{--}10^5 \text{ cm}^{-3}$ inferred for the small-scale H II regions. In determining the cooling function of the medium, we have used results that assume a solar abundance. The metallicity in the GC could be as much as twice solar, leading to an increased cooling efficiency.

The third difficulty is that the required value for l_0 in this model, $l_0 \sim 3 \times 10^{11} \text{ cm}$, is considerably smaller than that in the Galactic disk. In the Galactic disk, a stringent lower limit on the outer scale is 10^{13} cm , and it may be as large as 10^{18} cm (Armstrong et al. 1995). Although the physics for the generation and maintenance of small-scale density fluctuations is not well

understood, we regard it as potentially troublesome that this model predicts such a small l_0 .

4.2.2. “Warm” Interfaces

X-ray observations have revealed a central, diffuse X-ray source with a (FWHM) size of 1.8×0.9 (Yamauchi et al. 1990). Frail et al. (1994) suggested that this X-ray emitting gas may be responsible for the scattering. Yusef-Zadeh et al. (1997) suggested that this X-ray emitting gas is also the magnetoionic medium responsible for the Faraday rotation toward G 359.54+0.18.

The density and temperature of this region are estimated at 0.05 cm^{-3} and $10^7\text{--}10^8 \text{ K}$. This region cannot itself be the host of the density fluctuations because of its low density, cf. equation (31). However, this gas appears spatially coincident with the central zone of intense molecular emission and presumably abuts cooler gas in the clouds. We modify Frail et al.’s (1994) proposal by identifying the interfaces where the GC molecular clouds are exposed to this ambient hot medium as the source of the scattering. We term these interfaces “warm” by analogy with McKee & Ostriker’s (1977) model for the ISM. In that model cold clouds immersed in a hot (10^6 K) medium have 10^4 K interfaces. In the GC densities and temperatures are 1–2 orders of magnitude higher, but we expect that clouds will still develop intermediate temperature interfaces.

This model suffers from two of the same difficulties as the previous model. The X-ray emitting gas and molecular clouds appear to be in rough pressure equilibrium with $P \sim 5 \times 10^6 \text{ K cm}^{-3}$ (Blitz & Spergel 1991). Even though there are supersonic motions *within* the clouds, the clouds themselves ($v \sim 10\text{--}100 \text{ km s}^{-1}$) are moving subsonically with respect to the hot medium ($c_{\text{sound}} \sim 1000 \text{ km s}^{-1}$). Taking pressure balance to extend throughout the interface region, we find a density $n_e \sim 5\text{--}50 \text{ cm}^{-3}$ for $T_e \sim 10^5\text{--}10^6 \text{ K}$. From our likelihood results, the temperature within these interfaces implies an outer scale of $l_0 \sim 10^{-6.5}\text{--}10^{-6} \text{ pc}$, which, in turn, implies an rms density, equation (31), of $\delta n_e \sim 10 \text{ cm}^{-3}$. However, the cooling capacity of this medium is only $10^{-20} \text{ erg cm}^{-3} \text{ s}^{-1}$. The predicted heating rate is $\Gamma \sim 10^{-13} \text{ erg cm}^{-3} \text{ s}^{-1}$.

The outer scale in this model remains troublesomely small. If the size of the interface region is set by thermal conduction, the portion of the interface with $T_e < 10^6 \text{ K}$ has a size $\lesssim 10^{-1} \text{ pc}$ (McKee & Cowie 1977). Clearly if not all of the interface contributes to the scattering better agreement would be obtained between l_0 and the interface size. Still, the outer scale remains an order of magnitude smaller than its lower limit in the Galactic disk.

One point in favor of this model is the distribution of the X-ray emitting gas as compared to that of the molecular clouds. The size of the X-ray emitting region is similar to the extent of the scattering region, approximately 1° . In contrast, the molecular cloud distribution extends over the range $-1^\circ \lesssim \ell \lesssim 2^\circ$. If the scattering traced massive stars within these molecular clouds, as the photoionized molecular cloud skins model suggests, the scattering should extend further in longitude than it does. In this respect, the lack of enhanced scattering for H₂O masers in Sgr B is particularly problematic.

We stress the importance, and probable uniqueness, of the high density in the GC. In the Galactic disk density fluctuations cannot be supported in media with $T_e \sim 10^6$ K, a position with both theoretical and limited observational support (Spangler 1991; Phillips & Clegg 1992). Similarly, recent VLBI observations of 5 pulsars show no evidence for an enhanced level of turbulence at the boundary of the Local Bubble (Cox & Reynolds 1987; Britton, Gwinn, & Ojeda 1996), potentially a local analog of an interface between a hot and cooler medium. However, the Local Bubble and ambient medium have densities a factor of 10^2 – 10^3 smaller than that in the GC.

In summary, we use our likelihood results, §3.4, to constrain host media for the scattering material. Potential media include the photoionized skins of molecular clouds or the interface regions between the clouds and the ambient X-ray emitting gas. There are difficulties with both models: Both models overpredict the outer scale and appear to have some trouble supporting the required level of density fluctuations. Although we have been unable to make an unambiguous identification of the scattering medium with either medium, we favor the interface model, in part, because it shows a better correspondence between the spatial distribution of scattering and proposed host medium.

4.3. Modification of the Taylor-Cordes Model

The TC93 model modelled the global distribution of free electrons in the Galaxy with four components: an extended component, an inner Galaxy component, a component confined to the spiral arms, and a component local to the Gum Nebula. We now extend the TC93 model to include a GC component² (cf. eqn. [11] of TC93):

$$\begin{aligned} n_e(x, y, z) = & n_1(R, z) + n_2(R, z) + \sum_{j=1}^4 n_{\text{arm},j}(x, y, z) + n_{\text{Gum}}(x, y, z) \\ & + n_{\text{GC}} g_{\text{GC}}(R) h_{\text{GC}}(z). \end{aligned} \quad (33)$$

The first four components are discussed at length in TC93. We focus on only the last component, that toward the GC.

Based on the estimate in equation (31) and our estimates for l_0 , we take $n_{\text{GC}} = 10 \text{ cm}^{-3}$. Our estimate for Δ_{GC} is $\Delta_{\text{GC}} = 150 \text{ pc}$. Heretofore, we have been treating the scattering region as a screen with sharp boundaries. It is more likely that the region has soft edges. We therefore adopt a radial dependence of

$$g_{\text{GC}}(R) = \exp \left[-(R/0.150 \text{ kpc})^2 \right]. \quad (34)$$

² As in TC93, the coordinate system has the x -axis directed parallel to $\ell = 90^\circ$, the y -axis toward $\ell = 180^\circ$, the z -axis toward $b = 90^\circ$, and $R = \sqrt{x^2 + y^2}$ is the Galactocentric radius.

The latitude (or z) dependence of the screen is less well constrained. For definiteness we take

$$h_{\text{GC}}(z) = \exp \left[-(z/0.075 \text{ kpc})^2 \right] \quad (35)$$

corresponding to $\psi_b = 0^\circ.5$. The resulting axial ratio for the electron density distribution is 0.5; the axial ratio for the X-ray distribution is also 0.5 and that of the molecular cloud distribution is 0.3 (Morris & Serabyn 1996).

In the TC93 model the relationship between the free electron density and the scattering measure produced by a line of sight of length ds through those electrons is $d\text{SM} \propto F n_e^2 ds$. The parameter F is

$$F = \frac{\zeta \epsilon^2}{f} \left(\frac{l_0}{1 \text{ pc}} \right)^2, \quad (36)$$

where ζ is the normalized variance of electron density fluctuations between cloudlets and their surroundings and ϵ and f are as in equation (5). Taking $\zeta \sim \epsilon \sim 1$, our estimates for l_0 imply $F \gtrsim 10^4$. Both of the models we have considered here have $f < 1$. For definiteness, we take $f \sim 0.1$, recognizing that this may be an upper limit on f . We therefore conclude $F \gtrsim 10^5$. For comparison, the parameter F has a value of 0.4 in the solar neighborhood, 6 in spiral arms, and 40 in the Galaxy's inner few kiloparsecs.

A value of $F \sim 10^5$ produces an SM comparable to that suggested by the scattering diameters of Sgr A* and the OH masers. Their scattering diameters require a line-of-sight weighted scattering measure of $S \approx 10^2 \text{ kpc m}^{-20/3}$. Our results suggest $\Delta_{\text{GC}} \approx 150 \text{ pc}$; correcting for the line-of-sight weighting, equation (6), implies that the GC has a scattering measure of $\text{SM} \sim 10^{5.5} \text{ kpc m}^{-20/3}$. Integrating the TC93 expression for $d\text{SM}$ through the GC, with $F \sim 10^5$, we find $\text{SM} \sim 10^6 \text{ kpc m}^{-20/3}$.

Since the GC component is so localized, only for lines of sight through the GC are the results of TC93 altered. In this direction, however, the TC93 model underpredicts various quantities by a large amount. In the TC93 model, GC pulsars have $\text{DM} \approx 600\text{--}800 \text{ pc cm}^{-3}$; we predict that the DM will be somewhat larger, $\text{DM} \approx 2000 \text{ pc cm}^{-3}$, with approximately 1500 pc cm^{-3} of that arising from the GC component itself. For comparison, the largest DM known is for PSR B1758–23 with $\text{DM} = 1074 \text{ pc cm}^{-3}$ (Manchester, D'Amico, & Tuohy 1985; Kaspi et al. 1993). Further, from Cordes & Lazio (1997) the temporal broadening of pulses from pulsars seen through this region will be $350 \nu_{\text{GHz}}^{-4} \text{ seconds}$, requiring high-frequency ($\nu \approx 10 \text{ GHz}$) periodicity searches to detect pulsations. Although the DM we predict for GC pulsars is substantial, the dispersion smearing across a 1 GHz bandpass at 10 GHz ($\approx 5 \text{ ms}$) is comparable to the pulse broadening, so that only a small number of filterbank channels, e.g., 16, would be necessary to combat the dispersion smearing.

4.4. Conclusions

We use a likelihood analysis to determine the following parameters of the GC scattering region: The GC-scattering region separation, Δ_{GC} ; the angular extent of the region, ψ_ℓ and ψ_b ; the outer scale on which density fluctuations occur, l_0 ; and the gas temperature, T_e .

- From the literature we have assembled a list of all sources toward the GC for which angular broadening has been measured. A subset of these sources is OH/IR stars, for which the spatial distribution about the GC is known. We construct a likelihood function for the angular broadening of OH/IR stars, utilizing this distribution, §3.1. Masers within approximately 1° of Sgr A* have diameters consistent with $\Delta_{\text{GC}} \approx 150$ pc (Fig. 4).
- The likelihood analysis of our source counts, §3.2, indicates that a deficit of sources occurs within approximately 1° of Sgr A* and is caused by a scattering region within 500 pc of Sgr A* (Fig. 6). The resulting scattering diameter, at least $20''$ at 1 GHz, causes extragalactic sources to be so broad as to be resolved out by our observations.
- H₂O masers in and an extragalactic source near Sgr B and an extragalactic source near Sgr C do not show the extreme scattering of sources closer to Sgr A*, indicating that the scattering region does not extend to more than 1° in longitude. The latitude extent of the scattering region is poorly constrained, but is no more than 1° .
- From the literature we have estimated the free-free emission and absorption toward five heavily scattered masers near Sgr A*. The likelihood function is dominated by the free-free emission. The relevant parameters, Δ_{GC} , l_0 , and T_e , are not independent for this likelihood and only the product $\Delta_{\text{GC}}^{-2} l_0^{2/3} T_e^{-1/2}$ can be constrained (Fig. 7).

The global likelihood, formed by multiplying the individual likelihoods, is shown in Fig. 8. The maximum likelihood estimates of the parameters are $\Delta_{\text{GC}} = 150$ pc, $0.5^\circ \leq \psi_\ell \lesssim 1^\circ$, and $l_0^{2/3} T_e^{-1/2} = 10^{-7}$ with l_0 in pc and T_e in K. The parameter ψ_b was not well constrained and we adopt $\psi_b = 0^\circ.5$. The close correspondence between Δ_{GC} and $\psi_\ell D_{\text{GC}}$ suggests that the scattering region encloses the GC.

The GC scattering region produces a 1 GHz scattering diameter of $90''$, if the region is a single screen, or $180''$, if the region wraps around the GC, as appears probable. We modify the Taylor-Cordes model for the Galactic distribution of free electrons in order to include an explicit GC component. We predict that pulsars seen through this region will have a dispersion measure of approximately 2000 pc cm⁻³, of which approximately 1500 pc cm⁻³ arises from the GC component itself, and suffer pulse broadening of $350 \nu_{\text{GHz}}^{-4}$ seconds; pulsations will be detected only for frequencies above 10 GHz (Cordes & Lazio 1997).

As host media for the scattering we consider the photoionized surface layers of molecular clouds and the interfaces between molecular clouds and the 10^7 K ambient gas. We identify the

host medium by requiring that it be sufficiently dense to support density fluctuations of the required magnitude. We are unable to make an unambiguous determination, but we favor the interface model which predicts that the scattering medium is hot ($T_e \sim 10^6$ K) and dense ($n_e \sim 10 \text{ cm}^{-3}$). The X-ray interface model also shows better spatial agreement, when compared to the photoionized skin model, with the region over which the scattering is observed. This model is summarized graphically in Fig. 9.

The GC scattering region is likely to be unique in the Galaxy, probably because it is a high-pressure environment and can sustain densities and temperatures much higher than in the Galactic disk.

We thank Z. Arzoumanian, D. Frail, M. Goss, H. van Langevelde, F. Yusef-Zadeh, D. Chernoff, P. Goldsmith, and T. Herter for helpful and illuminating discussions. We thank N. Bartel for contributing additional angular broadening measurements. We thank the referee for a suggestion that helped improve the discussion of the likelihoods. This research made use of the Simbad database, operated at the CDS, Strasbourg, France. This research was supported by the NSF under grant AST 92-18075 and AST 95-28394. The NAIC is operated by Cornell University under a cooperative agreement with the NSF. TJWL holds a National Research Council-NRL Research Associateship. Basic research in astronomy at the Naval Research Laboratory is supported by the Office of Naval Research.

REFERENCES

Anantharamaiah, K. R., Pedlar, A., Ekers, R. D., & Goss, W. M. 1991, MNRAS, 249, 262

Armstrong, J. W., Rickett, B. J., & Spangler, S. R. 1995, ApJ, 443, 209

Backer, D. C., Zensus, J. A., Kellermann, K. I., Reid, M., Moran, J. M., & Lo, K. Y. 1993, Science, 262, 1414

Backer, D. C. 1988, in Radio Wave Scattering in the Interstellar Medium, eds. J. M. Cordes, B. J. Rickett, & D. C. Backer (New York: AIP) p. 111

Backer, D. C. 1978, ApJ, 222, L9

Becker, R. H., White, R. L., Helfand, D. J., & Zoonematkermani, S. 1994, ApJS, 91, 347

Becker, R. H., White, R. L., McLean, B. J., Helfand, D. J., & Zoonematkermani, S. 1992, ApJ, 358, 485

Beckert, T., Duschl, W. J., Mezger, P. G., & Zylka, R. 1996, A&A, 307, 450

Blitz, L. & Spergel, D. N. 1991, Nature, 379, 631

Britton, M. C., Gwinn, C. R., & Ojeda, M. J. 1996, ApJ, submitted

Churchwell, E. 1990, A&A Rev., 2, 79

Coles, W. A., Rickett, B. J., Codona, J. L., & Frehlich, R. G. 1987, ApJ, 315, 666

Condon, J. J., Broderick, J. J., & Seielstad, G. A. 1991, AJ, 102, 2041

Cordes, J. M. & Lazio, T. J. W. 1997, ApJ, 475, 557

Cordes, J. M., Weisberg, J. M., Frail, D. A., Spangler, S. R., & Ryan, M. 1991, Nature, 354, 121

Cordes, J. M., Clegg, A., & Simonetti, J. 1990, in Galactic and Intergalactic Magnetic Fields, eds. R. Beck, P. P. Kronberg, & R. Wielebinski (Dordrecht: Kluwer) p. 57

Cordes, J. M., Weisberg, J. M., & Boriakoff, V. 1985, ApJ, 288, 221

Cox, D. P. & Reynolds, R. J. 1987, ARA&A, 25, 303

Dalgarno, A. & McCray, R. A. 1972, ARA&A, 10, 375

Davies, R. D., Walsh, D., & Booth, R. S. 1976a, MNRAS, 177, 319

Davies, R. D., Walsh, D., Browne, I. W. A., Edwards, M. R., & Noble, R. G. 1976b, Nature, 261, 476

Dickey, J. M., Kulkarni, S. R., van Gorkom, J. H., & Heiles, C. 1983, ApJS, 53, 591

Frail, D. A., Diamond, P. J., Cordes, J. M., & van Langevelde, H. J. 1994, *ApJ*, 427, L43

Frail, D. A., Kulkarni, S. R., & Vasisht, G. 1993, *Nature*, 365, 136

Genzel, R., Hollenbach, D., & Townes, C. H. 1994, *Rep. Prog. Phys.*, 57, 417

Goldreich, P. & Sridhar, S. 1995, *ApJ*, 438, 763

Gray, A. D., Nicholls, J., Ekers, R. D., & Cram, L. E. 1995, *ApJ*, 448, 164

Gray, A. D., Whiteoak, J. B. Z., Cram, L. E., & Goss, W. M. 1993, *MNRAS*, 264, 678

Güsten, R. 1989, in *The Center of the Galaxy*, ed. M. Morris (Dordrecht: Kluwer) p. 89

Gredel, R. 1996, *The Galactic Center* (San Francisco: ASP)

Gwinn, C. R., Moran, J. M., Reid, M. J., & Schneps, M. H. 1988, *ApJ*, 330, 817

Handa, T., Sofue, Y., Nakai, N., Hirabayashi, H., & Inoue, M. 1987, *PASJ*, 39, 709

Helfand, D. J., Zoonematkermani, S., Becker, R. H., & White, R. L. 1992, *ApJS*, 80, 211

Higdon, 1986, *ApJ*, 309, 342

Higdon, 1984, *ApJ*, 285, 109

Isaacman, R. 1981, *A&AS*, 43, 405

Kaspi, V. M., Lyne, A. G., Manchester, R. N., Johnston, S., D'Amico, N., & Shemar, S. L. 1993, *ApJ*, 409, L57

Katgert, P., Oort, M. J. A., & Windhorst, R. A. 1988, *A&A*, 195, 21

Krichbaum, T. P. et al. 1993, *A&A*, 274, L37

Lazio, T. J. W. & Cordes, J. M. 1997, *ApJS*, submitted (Paper I)

Lazio, T. J. W., Spangler, S. R., & Cordes, J. M. 1990, *ApJ*, 363, 515

Lee, L. C. 1977, *ApJ*, 218, 468

Lindqvist, M., Habing, H. J., & Winnberg, A. 1992, *A&A*, 259, 118

Manchester, R. N., D'Amico, N., & Tuohy, I. R. 1985, *MNRAS*, 212, 975

Matthews, H. E., Davies, R. D., & Pedlar, A. 1973, *MNRAS*, 165, 173

McKee, C. F. & Cowie, L. L. 1977, *ApJ*, 211, 213

McKee, C. F. & Ostriker, J. P. 1977, *ApJ*, 218, 148

Mehringer, D. M., Palmer, P., Goss, W. M., & Yusef-Zadeh, F. 1993, *ApJ*, 412, 684

Mezger, P. G. & Pauls, T. 1979, in *The Large-Scale Characteristics of the Galaxy*, ed. W. B. Burton (Dordrecht: Reidel) p. 357

Minter, A. H. & Spangler, S. R. 1996, *ApJ*, 458, 194

Molnar, L. A., Mutel, R. L., Reid, M. J., Johnston, K. J., 1995, *ApJ*, 438, 708

Montgomery, D., Brown, M. R., & Matthaeus, W. H. 1987, *J. Geophys. Res.*, 92, 282

Moran, J. M., Rodríguez, L. F., Greene, B., Backer, D. C. 1990, *ApJ*, 348, 150

Morris, M. & Serabyn, E. 1996, *ARA&A*, 34, 645

Ozernoi, L. M. & Shishov, V. I. 1977, *Pis'ma Astron. Zh.*, 3, 435 (Sov. Astron. Lett., 3, 233)

Pedlar, A., Anantharamaiah, K. R., Ekers, R. D., Goss, W. M., van Gorkom, J. H., Schwarz, U. J., & Zhao, J.-H. 1989, *ApJ*, 342, 769

Phillips, J. A. & Clegg, A. W. 1992, *Nature*, 360, 137

Rickett, B. J. 1990, *ARA&A*, 28, 561

Rogers, A. E. E. et al. 1994, *ApJ*, 434, L59

Simonetti, J. H. & Cordes, J. M. 1986, *ApJ*, 303, 659

Skinner, G. K. 1993, *A&AS*, 97, 149

Spangler, S. R. 1991, *ApJ*, 376, 540

Spangler, S. R. & Gwinn, C. *ApJ*, 353, L29

Sridhar, S. & Goldreich, P. 1994, *ApJ*, 432, 612

Taylor, J. H. & Cordes, J. M. 1993, *ApJ*, 411, 674 (TC93)

van Langevelde, H. J., Frail, D. A., Cordes, J. M., & Diamond, P. J. 1992, *ApJ*, 396, 686

van Langevelde, H. J. & Diamond, P. J. 1991, *MNRAS*, 249, 7

White, R. L., Becker, R. H., Helfand, D. J., & Gregg, M. D. 1997, *ApJ*, 475, 479

Windhorst, R., Mathis, D., & Neuschaefer, L. 1990, in *Evolution of the Universe of Galaxies*, eds. R. Kron (San Francisco: ASP) p. 389

Yamauchi, S., Kawada, M., Koyama, K., Kunieda, H., & Tawara, Y. 1990, *ApJ*, 365, 532

Yusef-Zadeh, F., Wardle, M., Parastaran, P. 1997, *ApJ*, 475, L119

Yusef-Zadeh, F., Cotton, W., Wardle, M., Melia, F., & Roberts, D. A. 1994, *ApJ*, 434, L63

Yusef-Zadeh, F., Morris, M., Slee, O. B., & Nelson, G. J. 1986, *ApJ*, 310, 689

Zhao, J., et al. 1992, *Science*, 255, 1538

Zoonematkermani, S., Helfand, D. J., Becker, R. H., White, R. L., & Perley, R. A. 1990, *ApJS*, 74, 181

Fig. 1.— Possible scattering geometries toward the Galactic center. The dark circle represents a GC source such as Sgr A*, and the lightly colored regions indicate possible configurations for the ionized gas responsible for the radio-wave scattering. In general, we shall approximate the scattering region by a single screen.

Fig. 2.— The diameter of an extragalactic source at 1.4 GHz seen through the scattering region in front of Sgr A* as a function of the distance of the scattering region from the Galactic center, Δ_{GC} . The dotted line indicates an extreme lower limit on Δ_{GC} as derived from the lack of free-free absorption toward Sgr A* at centimeter wavelengths. At 1.4 GHz, the scattering diameter of Sgr A* is $0''.7$. The scattering diameter scales as $\theta_s \propto \nu^{-2}$.

Fig. 3.— Angular broadening measurements toward the GC compiled from Paper I and the literature. Crosses show the relative diameter of the major and minor axes of sources with measured angular diameters. The large star shows the relative size of the upper limit on the scattering diameter of the extragalactic source GPSR 0.539+0.263. Source diameters are scaled up by a factor of 500. The contours are from the 5 GHz survey with the NRAO 91 m telescope (Condon, Broderick, & Seielstad 1991).

Fig. 4.— $\mathcal{L}_{\text{broaden}}$, the likelihood function from angular broadening measurements on OH masers as a function of Δ_{GC} and ψ_ℓ . Contours show the 67% (*heavy*), 90%, and 99% confidence regions.

Fig. 5.— $\mathcal{L}_{\text{counts}}$, the likelihood function as a function of Δ_{GC} for the fields 359.9+0.2 (*solid*, 15' from Sgr A*), 358.9+0.5 (*dashed*, 77' from Sgr A*), and 358.1–0.0 (*dot-dash*, 113' from Sgr A*). These likelihood functions were all computed using Method 3, which uses our observations to estimate the number of Galactic sources in each field. Also shown is the likelihood function for the field 359.9+0.2 (*dotted*) in which only the number of extragalactic and unidentified sources is compared to the number of extragalactic sources expected. The discontinuity occurs where the number of detectable extragalactic sources becomes non-zero.

Fig. 6.— $\mathcal{L}_{\text{counts}}$, the likelihood function from source counts as a function of Δ_{GC} and ψ_ℓ . Contours show the 67% (*heavy*), 90%, and 99% confidence regions.

Fig. 7.— \mathcal{L}_{ff} , the likelihood function from free-free emission and absorption measurements as a function of Δ_{GC} and $l_0^{2/3} T_e^{-1/2}$. This likelihood is dominated by the free-free emission measurements. Contours show the 67% (*heavy*), 90%, and 99% confidence regions.

Fig. 8.— The global likelihood for GC scattering. Contours show the 67%, 90%, and 99% confidence regions. We assume $\psi_b = 0.5$. (a) \mathcal{L} as a function of Δ_{GC} and ψ_ℓ . The sharp edges in the contours reflect the underlying granularity of the data. (b) \mathcal{L} as a function of Δ_{GC} and $l_0^{2/3} T_e^{-1/2}$, with l_0 in pc and T_e in K. The maximum likelihood occurs at $\log l_0^{2/3} T_e^{-1/2} = -7.0$ and $\log \Delta_{\text{GC}} = -0.88$.

Fig. 9.— A graphical summary of the Galactic center scattering region (not to scale). The lightly colored region is the FWHM extent of the X-ray emitting (10^7 K) gas. The heavily colored regions are the molecular clouds (10^2 K), which are surrounded by the scattering gas (10^6 K). The central object is Sgr A* and the + signs represent some of the OH/IR stars.

Table 1. Angular Diameter Measurements from the Literature

Name	$\theta_{\text{obs}}^{\text{a}}$ (milliarcsecond)	$\Delta\Theta_{\text{Sgr A}^*}$ ($''$)	Ref.
OH 353.298–1.537	935	408.6	5
OH 355.641–1.742	855	277.5	5
OH 355.897–1.754	904	263.5	5
OH 357.849+9.744	408	600.6	5
OH 359.140+1.137	699	85.8	5
OH 359.517+0.001	2130	25.8	6
OH 359.564+1.287	232	83.2	5
OH 359.581–0.240	1680	24.7	6
OH 359.762+0.120 ^b	1710	14.8	6
OH 359.880–0.087	2760	4.6	6
OH 359.938–0.077	1480	1.9	3
OH 359.954–0.041	1540	0.7	3
OH 359.986–0.061	2460	2.6	6
OH 0.125+5.111	100	309.6	5
OH 0.190+0.036	268	15.6	3

Table 1—Continued

Name	$\theta_{\text{obs}}^{\text{a}}$ (milliarcsecond)	$\Delta\Theta_{\text{Sgr A}^*}$ ($''$)	Ref.
OH 0.319–0.040	3120	22.5	6
OH 0.334–0.181	3160	24.7	6
OH 0.892+1.342 ^c	163	100.9	5
OH 1.369+1.003	291	106.2	5
OH 1.212+1.258	670	109.1	5
OH 3.234–2.404	366	242.8	5
OH 5.026+1.491	194	318.5	5

Table 1—Continued

Name	$\theta_{\text{obs}}^{\text{a}}$ (milliarcsecond)	$\Delta\Theta_{\text{Sgr A}^*}$ ($''$)	Ref.
Sgr A*	1300	0.0	7
GCT	1310	0.6	4
A 1742–28	1380	0.9	1
Sgr B2(N)	276	45	5
GPSR 0.539+0.263	<3900	40	8

^aAll diameters are scaled to 1 GHz assuming a λ^2 scaling. For sources with anisotropic scattering disks, we quote the geometric mean of the semi-major and -minor axes.

^bFrail et al.’s (1994) diameter, also observed by van Langevelde & Diamond (1991) and van Langevelde et al. (1992)

^cvan Langevelde et al.’s (1992) diameter; Frail et al. (1994) cite difficulties with their fitting algorithm.

References. — (1) Davies et al. (1976a); (2) Gwinn et al. (1988); (3) van Langevelde & Diamond (1991); (4) Zhao et al. (1991); (5) van Langevelde et al. (1992); (6) Frail et al. (1994); (7) Yusef-Zadeh et al. (1994); (8) Bartel (1996, private communication)

Table 2. Source Counts and Expected Source Numbers

Field	1.28 GHz				1.66 GHz			
	N_{Gal}	N_{xgal}	N_{unid}	$\langle N_{\text{xgal}} \rangle$	N_{Gal}	N_{xgal}	N_{unid}	$\langle N_{\text{xgal}} \rangle$
357.9–1.0	0	2	9	5.1	0	1	9	5.2
358.1–0.0	3	0	13	5.8	1	0	16	6.9
358.7–0.0	2	1	19	3.4	2	1	17	4.0
358.9+0.5	0	1	12	5.4	0	1	10	6.6
359.9+0.2	1	0	1	7.5	20	0	1	1.1
0.0+0.0	20	0	1	0.4	28	0	1	3.2
0.2–0.7	0	0	14	2.7	0	0	13	6.7
0.5+0.2 ^a	0	0	16	7.8	0	0	22	8.5
1.0+1.6	0	0	15	9.7	0	0	14	11.0
1.2–0.0	1	0	3	2.2	1	0	5	3.9

^aExtent of field limited to avoid Sgr B.

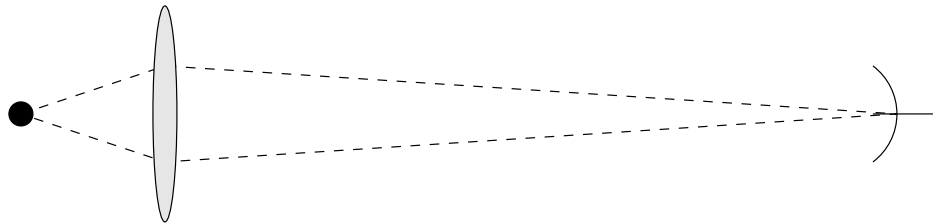
Table 3. Free-Free Emission Toward Heavily Scattered OH Masers

Name (1)	$\Delta\Theta_{\text{Sgr A}^*}$ ($'$) (2)	$\theta_{1.6 \text{ GHz}}$ ($''$) (3)	T_{ff} (K) (4)
OH 359.517+0.001	25.8	0.82	0.19
OH 359.581–0.240	24.7	0.64	0.11
OH 359.762+0.120	14.8	0.53	0.14
OH 0.319–0.040	22.5	1.20	0.48
OH 0.334–0.181	24.7	1.22	0.27

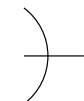
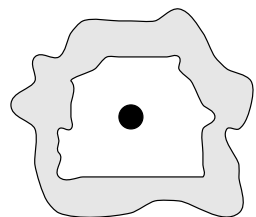
Note. — (2) Angular separation between maser and Sgr A*; (3) Angular diameter at 1.612 GHz, geometric mean of major and minor axis for those masers with anisotropic scattering disks, the scattering disk of Sgr A* at 1.612 GHz is $0''5$; (4) Brightness temperature at 10 GHz, from Handa et al. (1987), corrected for non-thermal emission.

SGR A*

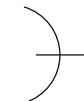
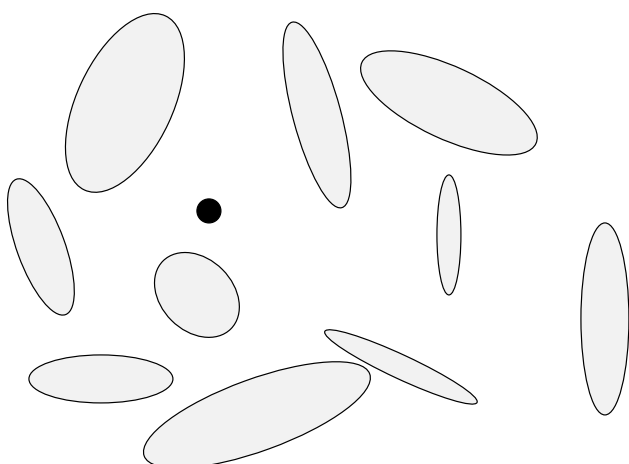
EARTH



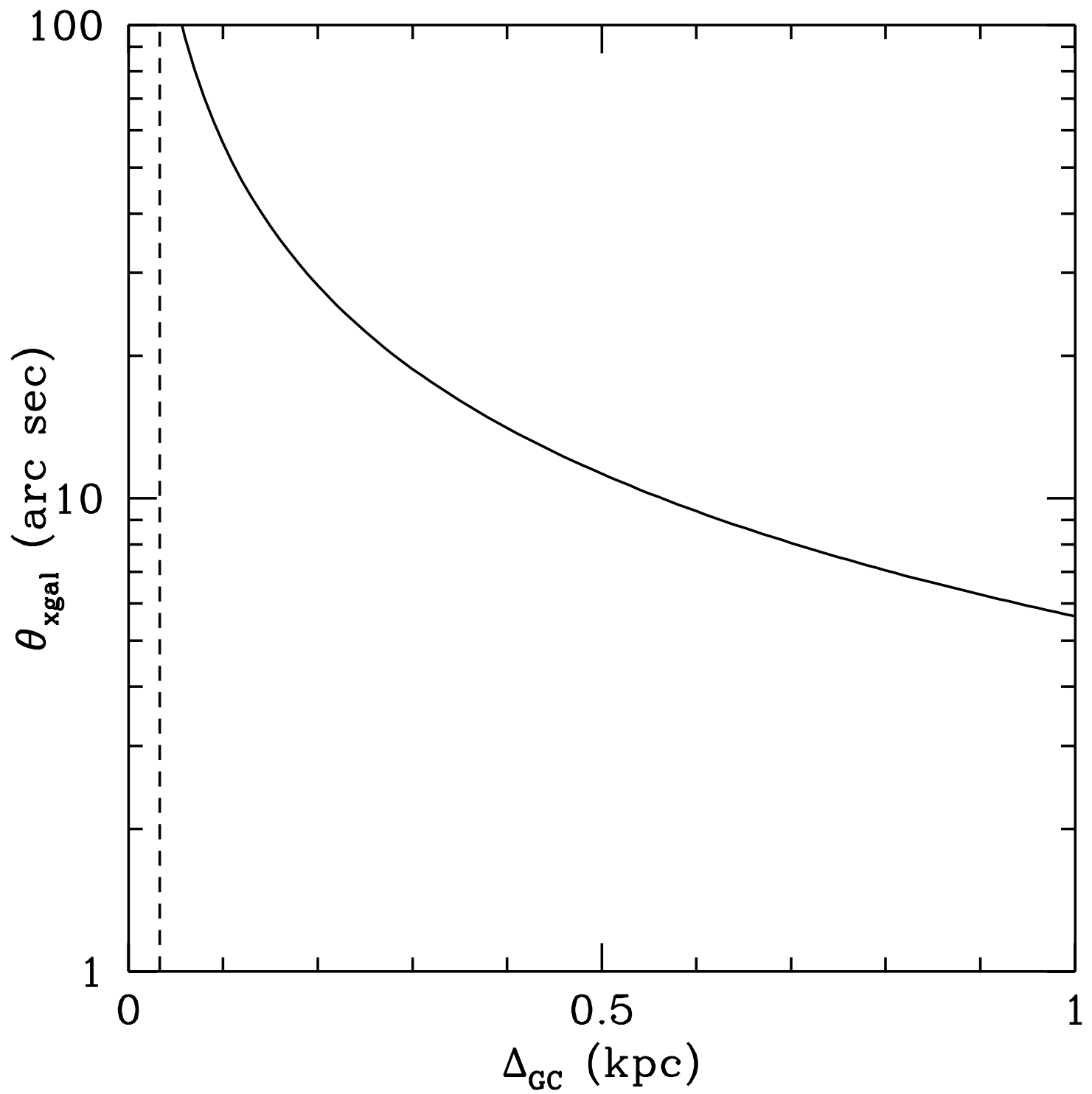
SINGLE SCREEN

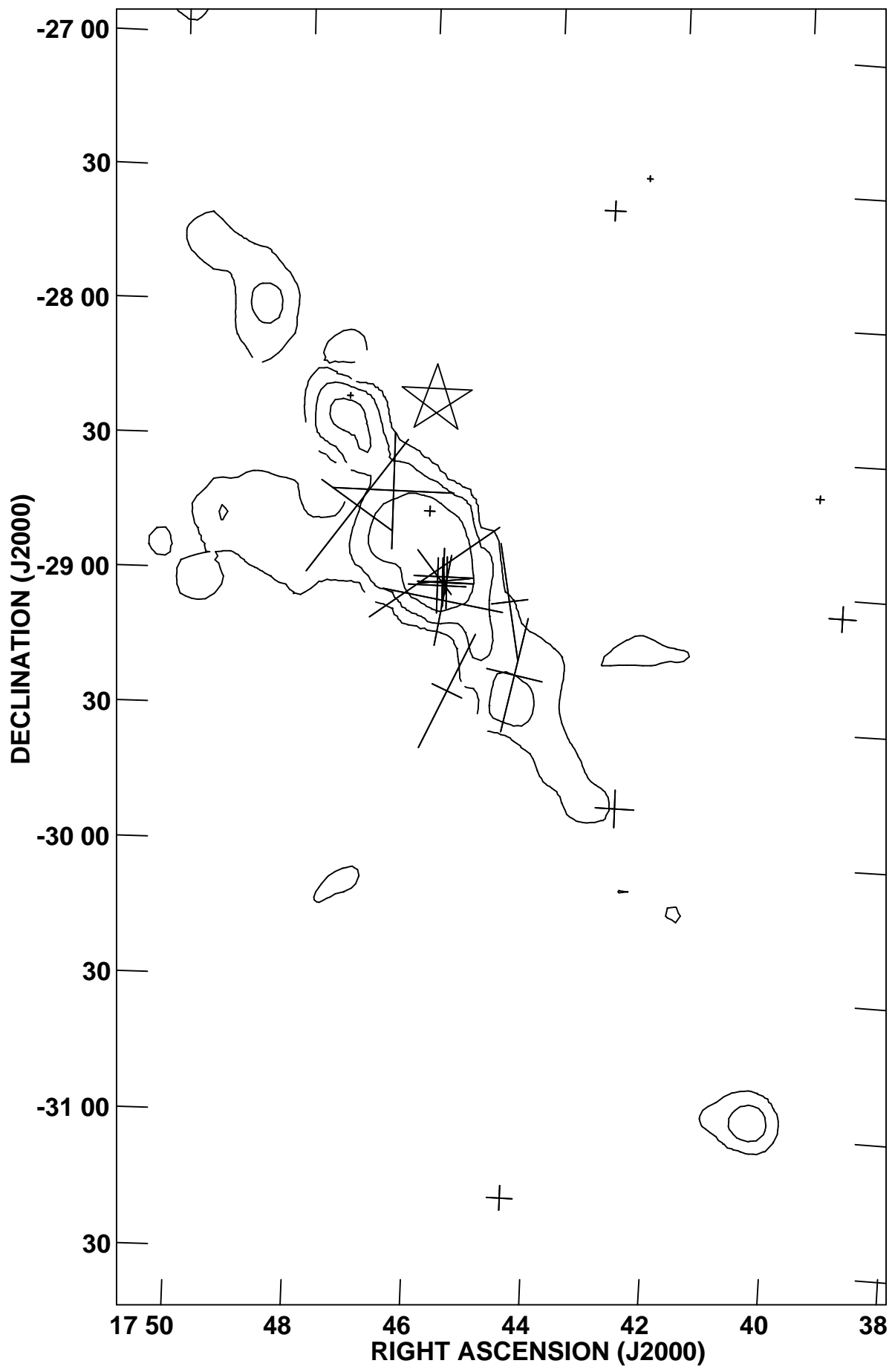


SHELL

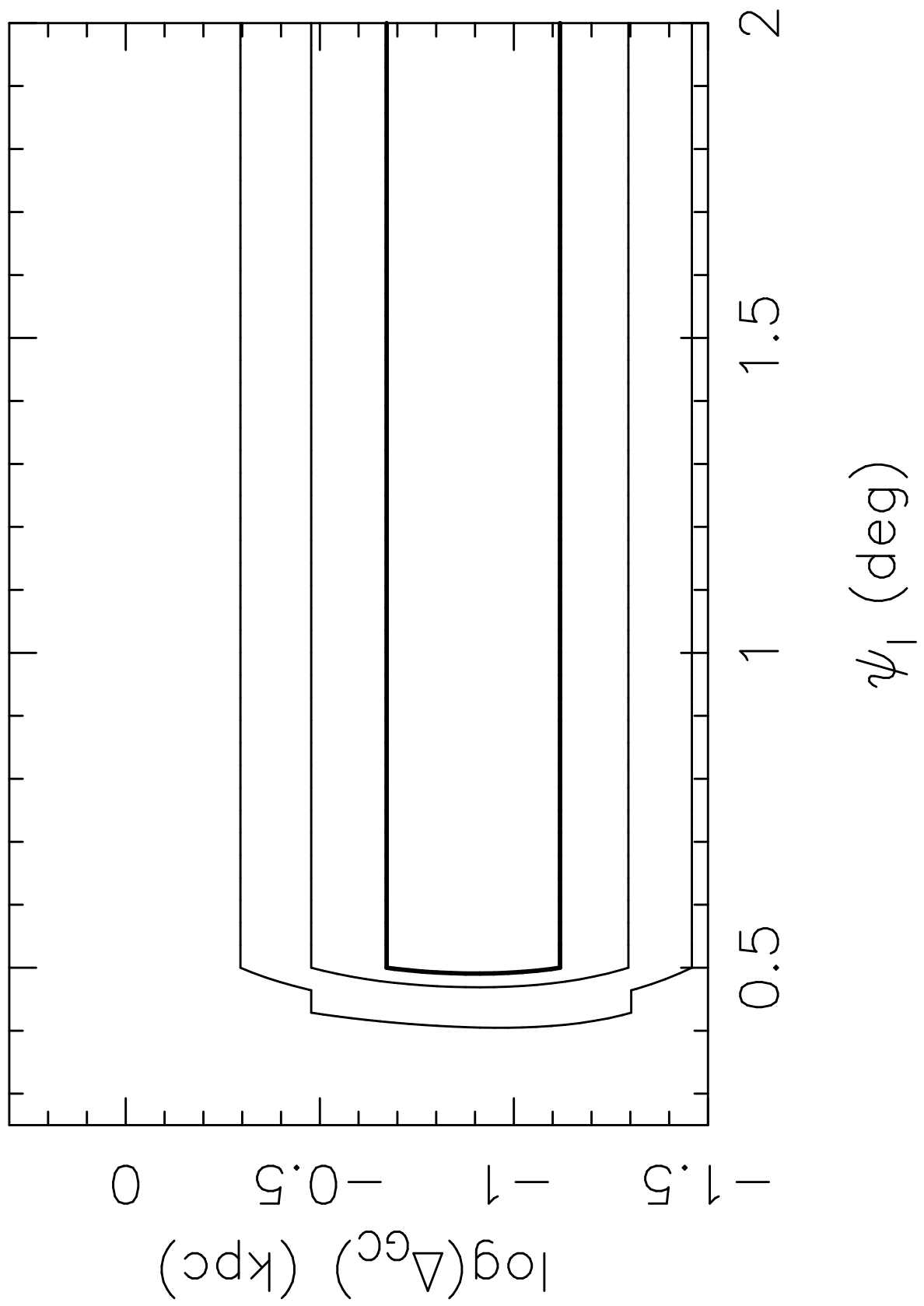


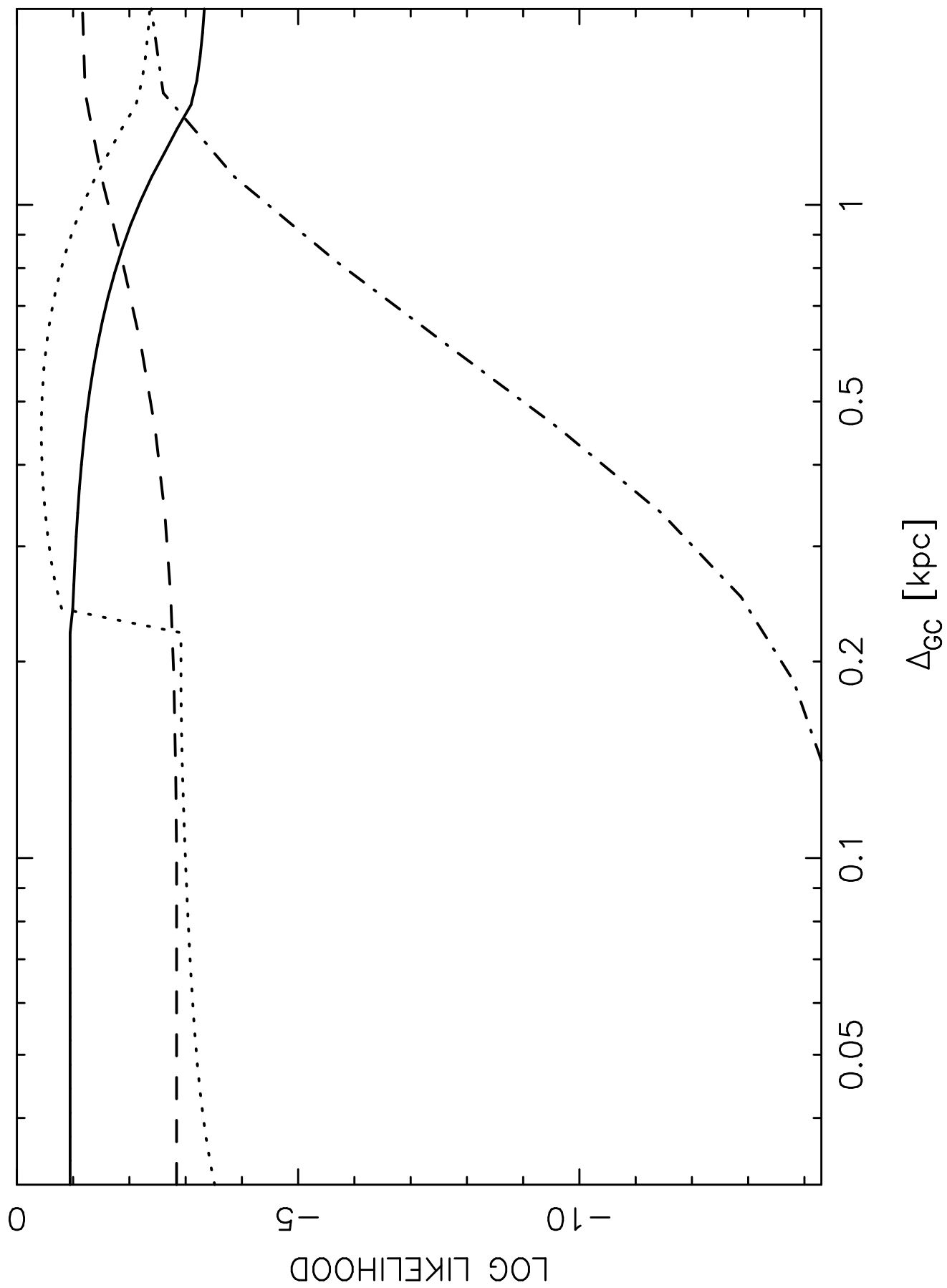
MULTIPLE SCREENS





$$\psi_b = 0.5^\circ$$





$$\psi_b = 0.5^\circ$$

